A General Framework for Process Synthesis, Integration, and Intensification

Salih Emre Demirel, Jianping Li, and M. M. Faruque Hasan*

Artie McFerrin Department of Chemical Engineering, Texas A&M University

College Station, TX 77843-3122, USA

Abstract

Process synthesis, integration and intensification are the three pillars of process design. Current synthesis and integration methods are able to find optimal design targets and process configurations when all the alternatives are known beforehand. Process intensification, on the other hand, combines multiple physicochemical phenomena and exploits their interactions to create innovative designs. Often times, these designs are not known beforehand, and a phenomena-level representation of chemical processes are required to identify them. This disconnection between the three paradigms limits the ability to systematically discover optimal design pathways. We demonstrate that the building block representation, originally proposed in our earlier work on process intensification (Demirel, Li and Hasan, Comput. Chem. Eng., 2017, 150, 2–38), has the potential to bridge this gap. Depending on the attributes assigned to the interior and the boundaries of these two-dimensional abstract building blocks, they can represent various intensified or isolated phenomena at the lowest level, various tasks at the equipment level, and various unit operations at the flowsheet level. This common multiscale representation enables an MINLP optimization-based single framework for the sequential or simultaneous synthesis, integration and intensification of chemical processes. Such a general framework is critical to reduce the risk of eliminating potential intensification pathways and candidate flowsheets at the conceptual design stage. The framework is demonstrated using a case study on ethylene glycol process.

Keywords: Process Intensification, Building Block Superstructure, Process Synthesis, Process Intensification, Ethylene Glycol

1 Introduction

Process design is the art and science of obtaining process flowsheets that are capable of converting a set of feedstocks into a set chemical products while meeting the product specifications in terms of both quality and quantity. A major goal of systematic design is to identify the equipment types, their configurations and operating conditions, and the connectivity that would result in optimal processing networks. Process synthesis, integration and intensification are the areas that addresses this goal at the conceptual design stage (Figure 1).

[Figure 1 about here]

Process synthesis aims at screening flowsheet variants, equipment types, operating conditions and equipment connectivity under several design and operational constraints. While early works on process synthesis utilized heuristics and hierarchical synthesis steps to generate flowsheet variants,[1–6] superstructure optimization-based synthesis approaches gained more attention owing to their systematic nature and the ability to screen numerous process configurations.[7–13] Process integration takes a holistic approach and aims at reducing the consumption of resources by increasing the internal recycling and reuse of energy and materials.[14,15] Pinch analysis and optimization-based methods are two common approaches for process integration.[15] There also exist hybrid approaches for process synthesis[16,17] and integration[18] that combine hierarchical decision-making with mathematical optimization to enable efficient screening of alternatives at multiple stages. These methodologies strive for overcoming the challenges posed by the inherent combinatorial complexity in process design.[19]

Process intensification is defined as any design activity that gives rise to significant improvement in performance metrics while yielding economically more favorable, more sustainable and safer operation.[20–22] This can be achieved via enhancement in driving forces for mass/heat/momentum transfer and/or surpassing the equilibrium limitations imposed by thermodynamics. There are several successful industrial applications of intensified technologies. These include reactive distillation columns, dividing wall columns, reverse flow reactors, static

*Correspondence concerning this article should be addressed to M.M. Faruque Hasan at hasan@tamu.edu, Tel.: 979-862-1449.

mixers, and rotating packed beds.[23] However, a wider application of process intensification in the chemical industry requires systematic tools that could suggest novel design alternatives at the early design stage.[24]

Whether it is process synthesis, integration or intensification, the focus is to design energy efficient, sustainable and cost-effective chemical processes. However, there are several differences between these approaches (Table 1). Traditional process synthesis activities operate at the equipment and flowsheet scales to find the optimal conditions and configurations. Process integration deals with plant-scale decisions, material/energy redistribution and utility networks. Process Intensification, on the other hand, seeks for enhancements at the fundamental physicochemical phenomena scale to generate novel equipment and flowsheet alternatives.[25]

[Table 1 about here]

These differences are also reflected in the mathematical models used in these methods. Process integration pivots around material and energy flows and source-sink connectivity. These models are sometimes simplistic.[26] In traditional process synthesis, equipment sizing and connectivity can be fairly represented using short-cut methods[27,28] and surrogate models.[29–31] Process intensification needs a more detailed description of physicochemical phenomena that are governed by the fundamental material/energy/momentum transport and thermodynamic constraints.[21]

Regardless of the dissimilarities, there is a symbiotic relationship that exists among the synthesis, integration and intensification activities. Baldea,[32] for instance, showed that intensification could be regarded as a limiting case of tight material integration. This relationship is also highlighted by Ponce-Ortega et al.[33] who suggested intensification at both the unit operations and the plant levels. Tight integration together with process synthesis can increase the sustainability and profitability, and in some cases, even lead to intensification through eliminating costly equipment, or utility streams.[34,35] This signifies the importance of considering them in tandem at the early stage of a design activity. The challenge, however, lies in formulating a general method that can combine process synthesis, integration and intensification in a single framework.

This generalization, most crucially, requires a common representation method that is amenable to relate the fundamental process constituents (phenomena) with the equipment and flowsheet configurations by capturing the synergies at different scales. One of the earliest works emphasizing this aspect came from Siirola,[36] who proposed means-end analysis that is based on the elimination of property differences between the raw materials and the products through task-based operators. The methodology is able to systematically transform a traditional methyl acetate process with standalone reactor and separation columns into an intensified process that simultaneously performs reaction, extraction and distillation operations in a single task-integrated column.[37] There are several works that depart from unit operation-based representation of process alternatives and employ a set of processing tasks, phenomena, or functions to identify new designs.[38–42] The leading approach in this vein is the phenomena-based design, where a chemical process is regarded as a combination of phenomena such as mixing, splitting, phase contact, phase change, reaction, heating, cooling, etc. In this approach, one seeks for novel designs by recombining these low-scale constituents in task-integrated equipment.

Gani and coworkers[25,43] developed a computer-aided comprehensive methodology for process synthesis-intensification based on phenomena-based building blocks (PBBs). In this method, several major PBBs are used to represent and recreate process flowsheets. The candidate phenomena are identified from an existing or base flowsheet, which are then screened for feasibility. The most promising phenomena-based structures are transformed into unit operations. Babi et al.[44] introduced a superstructure-based approach for the selection of the base flowsheets. Kuhlmann et al.[45] proposed to use PBBs within a state-space superstructure representation for synthesizing intensified process flowsheets. There are other bottom-up approaches besides the knowledge-based phenomena representation. Pistikopoulos and coworkers[46,47] proposed a Generalized Modular Framework (GMF) for the representation of chemical processes based on multifunctional mass/heat exchange modules. Manousiouthakis and co-workers proposed Infinite DimEnsionAl State Space (IDEAS) framework[48,49] as a synthesis tool for process intensification.

Phenomena-based approaches are promising in terms of establishing a common platform for process synthesis, integration and intensification. This has not been achieved yet because

of the lack of a common representation that can combine multiple scales representing the phenomena, tasks and unit operations in a seamless fashion. Recently, our group has proposed a unique representation based on abstract building-blocks[50] for optimization-based systematic process intensification, which shows promise to fill this gap. These building blocks decompose classical unit operations into different phenomena and tasks, and seek for intensified equipment and flowsheets through optimal recombination.[50,51] We have showed the merits of this representation for automatic flowsheet generation in process synthesis.[52–54] We have also applied the representation for addressing different process integration problems, including mass, heat and property integration.[54–57] In these works, a superstructure of two-dimensional abstract building blocks has been used.

In this work, we employ the unique features of the building block-based representation toward developing a common platform for process synthesis, integration and intensification. Based on this representation, a general modeling framework is proposed that can capture various phenomena models with differing details. The remainder of the article is structured as follows. First, we present the generic features of the building block representation. Next, we formalize the problem statement and describe a mixed-integer nonlinear optimization (MINLP) formulation for general process synthesis, integration, and intensification. Lastly, we demonstrate the applicability of the framework using a case study on the synthesis, integration and intensification of an ethylene glycol process.

2 Representation using Building-Blocks

The proposed unified framework is based on a new representation of chemical processes using two-dimensional building blocks[50,52,55] that are abstract modules with interiors and four boundaries as the fundamental design elements. Each building block stands for either a physicochemical phenomena (e.g. mixing, reaction, splitting, etc.), a processing task (e.g., compression, expansion, etc.), a chemical equipment (e.g. a PFR reactor), or a simple empty block without any assignment. Regardless of the assignment, building blocks share some common features that are illustrated in Figure 2. Each building block has temperature, pressure and composition attributes, denoted by T, P, and y, respectively. Our goal is to identify the optimal

values of these physical qualities and thermodynamics as well as the optimal phase assignments for each block while considering the appropriate thermodynamic relations between the attributes. There can be multiple incoming and outgoing streams through the block boundaries which are described by their flow rate, temperature, pressure and composition. All outgoing streams from a block share the same temperature and pressure (Figure 2a). Chemical transformations and changes in the component qualities are represented inside the block. This means that incoming material streams to a building block are assumed to be mixed before getting involved in a transformation. This mixing is based on linear relationships in terms of the material flows, but other mixing rules can be applied as well. Representing chemical transformations within the block implies that the stream composition stays the same after it leaves the source block.

[Figure 2 about here]

In describing different elements of the chemical processes multiple blocks might be required. In this case, the interaction of the building blocks between each other becomes important. These interactions are enabled through the boundary separating two blocks from each other (Figure 2b). Each boundary between two neighboring blocks is classified as either unrestricted, semirestricted or completely restricted (Figure 2c) to capture different patterns of interactions in chemical processes. Unrestricted boundary indicates that the flow through it has the same composition with its source block. There is no mass transfer interception between the neighboring blocks sharing a common unrestricted boundary. Completely restricted boundary is used to describe zero-flow conditions. Semirestricted boundary designates that the stream leaving through this boundary has a different composition than the source block itself. Two neighboring blocks with a common semirestricted boundary may represent a separation operation. If one block is in vapor phase and the other is in liquid phase, then a semirestricted boundary indicates a phase boundary between these phases.

At a lower level, building blocks stand for a single or combination of multiple physicochemical phenomena that form a chemical process. Examples of these phenomena are reaction, phase contact and transition, mixing, splitting, heating, cooling, etc.[25] By using multiple building blocks, many of these physicochemical phenomena can be represented. This is illustrated in Figure 3a. While mixing, splitting, reaction, heating and cooling phenomena can be represented

by only one block, phase contact and phase transition are represented by at least two neighboring blocks with different phases. Combination of building blocks can be also used to realize more complex phenomena. For instance, a block holding a liquid mixture in contact of its vapor phase together represent a V-L phase equilibrium. If reaction also takes place in the liquid phase, then these two blocks represent a reactive flash operation or a part of a reactive separation column. An evaporation (condensation) operation with heating (cooling) can be represented using a unidirectional phase transition and material flow from one block to another. And, when all the building blocks are connected to each other, as shown in Figure 3b as an example, an intensified column with reactive and non-reactive sections is obtained.

[Figure 3 about here]

At a higher level, a building block can also be used to emulate a single chemical equipment, such as a distillation column or a plug-flow reactor. In this case, the overall operation of the unit is described by a single block instead of multiple blocks. Several examples of these unit operation-based representations are shown in Figure 4. In representing separation equipment, semirestricted boundary is utilized (Figure 4a). Each separation equipment requires at least one rich and one lean outlet stream with different compositions in terms of a key component. A semirestricted boundary indicates the position of one of these streams. A reactor unit is represented by a single block (Figure 4b). With appropriate input-output models, most equipment can be represented using a single block (Figure 4c). To enrich the representation further, each stream is embedded with a temperature and/or pressure manipulator, as shown in Figure 4d-e.

By comparing Figures 3 and 4, we observe that building blocks describing different physicochemical phenomena can capture an intensified unit with reactive/non-reactive sections, side-heaters and coolers. However, equipment-based representation lack this flexibility. When we represent an equipment with a single building block, we fix the equipment-type and configuration.

[Figure 4 about here]

These building block definitions for physicochemical phenomena and equipment lays the foundation for a unified representation for process synthesis, integration and intensification.

Various features of synthesis, integration and intensification are summarized in Table 1. To realize them in a single framework, we need a common representation of the problem. This superstructure representation is accomplished by collecting the building blocks in a two-dimensional (2D) grid as shown in Figure 5a. This 2D formation allows for systematic representation of many alternative design pathways as elaborated below.

[Figure 5 about here]

Each block $B_{i,j}$ is denoted with its position in the grid. Where $i = 1, ..., I$ denotes the rows, $j = 1, ..., J$ denotes the columns (Figure 5a). Then, the basic block variables shown in Figure 2 can be indexed according to the position of the blocks. The connectivity within the superstructure is captured through inter-block streams and jump streams. Inter-block streams, shown as directed arrows in Figure 5a, can go through all four boundaries surrounding the block and flow in either direction to allow reverse flow. These flows are denoted as $F_{i,j,k,d}$ in Figure 5b. Component set $k = 1, ..., K$ includes all the chemical species involved in the system. Direction set indicates whether a stream is flowing in horizontal ($d = 1$) or vertical ($d = 2$) direction. A flow between block $B_{i,j}$ and $B_{i,j+1}$ in horizontal direction, is denoted as $F_{i,j,k,d=1}$. It is $F_{i,j,k,d=2}$ when between blocks $B_{i,j}$ and $B_{i+1,j}$. If this variable has positive value, then the flow is from block $B_{i,j}$ to $B_{i,j+1}$. If it is negative, then the flow direction is reversed. Jump streams can connect non-adjacent blocks to each other and these streams increase the connectivity within the superstructure. Jump flows are denoted as $J_{i,j,i',j',k}$ to indicate the flow of component k from block $B_{i,j}$ to $B_{i',j'}$ (shown on the left upper and right lower corners of the block in Figure 5b). Each block can take materials from outside the system boundaries via the external feed streams and send out product streams. External feed streams are allowed to enter the superstructure with a flow rate $M_{i,j,k,f}$ indicating the amount of component k in feed stream ($f = 1, .., FS$) entering into the block $B_{i,j}$. Similarly, product streams can be taken out from any block as $P_{i,j,k,ps}$ ($ps = 1, .., PS$). $G_{i,j,k}$ refers to generation or consumption of component k in $B_{i,j}$. Energy flow within the superstructure (Figure 5c) is facilitated through the stream enthalpies and heat introduced or withdrawn by external utility streams. Heat from these external utilities is either transfered to the block itself or to the stream heaters. Similarly, pressure change is satisfied through the stream compressors/expanders/pumps/valves (Figure 5d). Energy flow

terms, as shown in 5c, include enthalpy carried out by the material streams, $EF_{i,j,d}$, including the external feed, $EM_{i,j,f}$ and products, $EP_{i,j,p}$, enthalpy of reaction, $EG_{i,j}$ and block heat duty variables, $Q^h_{i,j}$ and $Q^c_{i,j}$.

Various process integration problems can be addressed with this generic superstructure representation. Blocks, inter-block streams and jump streams can be used to represent source-sink interactions and connectivity between them. A simple source-sink network example is given in Figure 6a for illustration. Four source streams and one sink can be represented by a single block with four feed streams and one product stream. In the flowsheet level, material integration can be realized as recycle streams. These recycle streams can be represented with both interblock and jump connections. This is shown in Figure 6b for a reactor-separator-recycle process. Block $B_{1,1}$ represents the reactor with the external feed and block $B_{2,2}$ stands for the separator. One outlet from the separator is taken to block $B_{2,3}$ through the semirestricted boundary which represent the bottoms of the separator. The other outlet stands for the top stream of this separator and it is recycled back to the reactor. By using interblock streams, this recycle is achieved through two interblock streams going through $B_{2,1}$. Here, blocks $B_{2,1}$ and $B_{1,2}$ are used only for material transfer and act as pipes for material transfer. Alternatively, this recycle stream can be represented as a single jump stream from block $B_{2,2}$ to $B_{1,1}$. In this case, less number of blocks are utilized to represent the same flowsheet.

Heat integration is achieved through matching the heat requirements of any stream heater/cooler or block heat duty with each other. This is shown in Figure 6c. If the utility requirement of a hot and cold stream at two different positions are the same, then they can be integrated to each other. If no such stream available, then the heating/cooling requirement is satisfied via external utilities. These matches can be also restricted to certain positions to obtain traditional heat exchanger network synthesis superstructures.[58]

[Figure 6 about here]

At lower levels of representation, building blocks can be used to address various process synthesis and intensification problems in a superstructure-based framework. All of these features are summarized in Figure 7. By merely utilizing the connectivity, a water network synthesis superstructure can be represented as given in Figure 7a. Here, the first row of the superstructure

corresponds to interceptor units in which source streams are mixed and processed. The second row represents the sink blocks where streams with different qualities are obtained. The connectivity between interceptors and sinks is satisfied via jump streams. When a single block is used to represent an equipment, traditional equipment-based process synthesis superstructures can be represented. This is illustrated in Figure 7b for a superstructure with two reactor alternatives where the reaction products separated by a distillation column and recycled back to the reactors. In the lowest level, phenomena-based description of building blocks opens up many possibilities for novel process design. This is illustrated in Figure 7c via a flowsheet featuring a reactive DWC (dividing wall column) followed by a pervaporation membrane operation. Here, a completely restricted boundary separates the two parts of the DWC from each other. Each part includes several stages of reactive vapor-liquid equilibrium building blocks. Top product from the DWC is sent to a pervaporation-based membrane operation. In this membrane unit, semi-restricted boundary between the permeate and retantate sides represents the membrane material.

[Figure 7 about here]

With these representation features, building block superstructure becomes a unified superstructure representation for process synthesis, integration and intensification. This generic representation can be also translated into a unified modeling framework. This unified model is described in the next section.

3 MINLP Model Formulation

In this section, a general mathematical formulation for process synthesis, integration and intensification is provided. Common features of the representation described in the previous section also translate into this model. A feasible superstructure connectivity requires material and energy balances to be satisfied for each block. Reaction operations and change in component qualities are modeled in the block. Splitting and separation operations are described through block boundary formulations. By using these, a general MINLP (Mixed Integer Nonlinear Programming) optimization formulation can be formulated. In this model, material and energy

flows are quantified through continuous variables. Position of the active operations (phenomena or equipment) in the grid is determined by discrete variables. When these binary variables are restricted to be active at pre-specified positions of the grid, a superstructure with reduced number of alternatives is obtained (As in Figure 7). If these binary variables are allowed to be active at any position in the grid, flowsheets can be automatically generated.

Several parameters and set descriptions are required for the MINLP model. Beside the grid dimension sets which determine the size of the superstructure, set $FS = \{f|f = 1, ..., |FS|\}$ of raw material/feeds streams with their maximum availability F_f^{feed}, a set $K = \{k|k = 1, ..., |K|\}$ of chemical species involved in the system, a set $RX = \{r|r = 1, ..., |RX|\}$ of chemical reactions, a set $C = \{cat|cat = 1, ..., |CAT|\}$ of catalysts or available reactor units, a set $s = \{s|s = 1, ..., |S|\}$ of separation equipment or phenomena, a set $m = \{m|m = 1, ..., |M|\}$ of enabling materials for the separation phenomena are given. Material properties, e.g. membrane permeability toward a chemical component, reaction stoichiometry, kinetic expressions, phase and reaction equilibrium parameters are assumed to be available. The objective of the problem is to synthesize a flowsheet or process network that maximizes the annual total profit/minimizes the total annual cost or operating costs and produce a set $PS = \{p|p = 1, ..., |PS|\}$ of products streams while satisfying their demand of D_p and satisfying maximum waste/emission requirement, where, $y_{k,p}^{MIN,prod}$ and $y_{k,p}^{MAX,prod}$ denote the minimum and maximum allowed concentration, respectively, for component k in product p.

Discrete variables required for determining the position of the active operations in the grid include the following boundary and block binary variables:

$$z_{i,j,d}^{un} = \begin{cases} 1 & \text{If } F_{i,j,k,d} \text{ is unrestricted} \\ 0 & \text{Otherwise} \end{cases}$$

$$z_{i,j,d}^{sr} = \begin{cases} 1 & \text{If } F_{i,j,k,d} \text{ is semi-restricted} \\ 0 & \text{Otherwise} \end{cases}$$

$$z_{i,j,d}^{cr} = \begin{cases} 1 & \text{If } F_{i,j,k,d} \text{ is completely restricted} \\ 0 & \text{Otherwise} \end{cases}$$

These variables are to classify the boundary type. When a boundary assigned as semirestricted, a specific type of separation operation or phenomena is also assigned to it. This is determined by the following binary variable:

$$z^{s}_{i,j,d,s,m} = \begin{cases} 1 & \text{If boundary is assigned with separation operation s and enabling material m} \\ 0 & \text{Otherwise} \end{cases}$$

Similarly, a reaction assignment binary variable is defined for each block:

$$z^{rxn}_{i,j,c} = \begin{cases} 1 & \text{If block is assigned with a reaction operation} \\ 0 & \text{Otherwise} \end{cases}$$

With this, we provide the unified MINLP model (P0) for process integration, synthesis and intensification below:

$$\max/\min \quad TAP$$

$$s.t. \quad F_{i,j-1,k,1} + F_{i-1,j,k,2} - \sum_{d\in D} F_{i,j,k,d} + G_{i,j,k} + M^{f}_{i,j,k} - P^{p}_{i,j,k} + J^{f}_{i,j,k} - J^{p}_{i,j,k} = 0 \tag{1}$$

$$M^{f}_{i,j,k} = \sum_{f\in FS} M_{i,j,k,f}; P^{p}_{i,j,k} = \sum_{p\in PS} P_{i,j,k,p} \tag{2}$$

$$J^{f}_{i,j,k} = \sum_{(i',j')\in LN} J_{i',j',i,j,k}; J^{p}_{i,j,k} = \sum_{(i',j')\in LN} J_{i,j,i',j',k} \tag{3}$$

$$M_{i,j,k,f} = F^{feed}_{f} y^{feed}_{k,f} z^{feedfrac}_{i,j,f} \tag{4}$$

$$y^{MIN,prod}_{k,p} \sum_{k'\in K} P_{i,j,k',p} \le P_{i,j,k,p} \le y^{MAX,prod}_{k,p} \sum_{k'\in K} P_{i,j,k',p} \tag{5}$$

$$\sum_{i\in I}\sum_{j\in J}\sum_{k\in K} P_{i,j,k,p} \ge D_p \tag{6}$$

$$F_{i,j,k,d} = FP_{i,j,k,d} - FN_{i,j,k,d} \tag{7}$$

$$EB^{in}_{i,j} - EB^{out}_{i,j} + \textstyle\sum_f EM_{i,j,f} - \sum_p EP_{i,j,p} + EG_{i,j} + Q^{h}_{i,j} - Q^{c}_{i,j} = 0 \tag{8}$$

$$\begin{aligned} &EF_{i,j,d} = f^{ent}(F,y,T,P); EF^{1}_{i,j,d} = f^{ent}(F,y,T,P); \\ &EF^{2}_{i,j,d} = f^{ent}(F,y,T,P), EJ_{i,j,i',j'} = f(J_{i,j,i',j',k}, T_{i,j}, P_{i,j}) \end{aligned} \tag{9}$$

$$Q^{F}_{i,j,d} = EF^{1}_{i,j,d} - EF_{i,j,d} \tag{10}$$

$$W^{F}_{i,j,d} = EF^{2}_{i,j,d} - EF^{1}_{i,j,d} \tag{11}$$

$$\phi_{i,j,k} = FP_{i,j-1,k,1} + FP_{i-1,j,k,2} + \sum_{d} FN_{i,j,k,d} + \sum_{f} M_{i,j,k,f} + \sum_{(i',j')\in LN} J_{i',j',i,j,k} \tag{12}$$

$$G_{i,j,k} = \sum_{(r,c)\in rxr} Re_{i,j,k,r,c} \tag{13}$$

$$\left[\begin{array}{c} z^{rxn}_{i,j,c} = 1 \\ Re_{i,j,k,r,c} = f^{rxn}(\gamma_{r,k}, Conv_{i,j,r,c}, \phi_{i,j,k}, T_{i,j}, P_{i,j}, y_{i,j,k}, V_{i,j}) \end{array} \right] \bigvee \left[\begin{array}{c} z^{rxn}_{i,j,c} = 0 \\ Re_{i,j,k,r,c} = 0 \end{array} \right] \tag{14}$$

$$y_{i,j,k} \sum_{k'\in K} P_{i,j,k',p} = P_{i,j,k,p}; y_{i,j,k} \sum_{k'\in K} J_{i,j,i',j',k'} = J_{i,j,i',j',k} \tag{15}$$

$$z^{un}_{i,j,d} + z^{sr}_{i,j,d} + z^{cr}_{i,j,d} = 1 \tag{16}$$

$$z^{sr}_{i,j,d} = \sum_{s\in S, m\in M} z^{s}_{i,j,d,s,m} \tag{17}$$

$$\left[\begin{array}{c} z^{un}_{i,j,d} = 1 \\ FP_{i,j,k,d} = y_{i,j,k} \sum_{k'\in K} FP_{i,j,k',d} \end{array} \right] \bigvee \left[\begin{array}{c} z^{un}_{i,j,d} = 0 \\ 0 \le F_{i,j,k,1} \le FU \end{array} \right] \tag{18}$$

$$\left[\begin{array}{c} z^{sr}_{i,j,d} = 1 \\ F_{i,j,k,1} = \\ f^{sr}(\phi_{i,j,k}, \tau_{i,j,k,d,s,m}, y_{i,j,k}, T_{i,j}, P_{i,j}, \\ T_{i,j+1}, P_{i,j+1}, y_{i,j,k}) \end{array} \right] \bigvee \left[\begin{array}{c} z^{sr}_{i,j,d} = 0 \\ 0 \le F_{i,j,k,1} \le FU \end{array} \right] \tag{19}$$

$$\left[\begin{array}{c} z^{cr}_{i,j,d} = 1 \\ F_{i,j,k,1} = 0 \end{array} \right] \bigvee \left[\begin{array}{c} z^{cr}_{i,j,d} = 0 \\ 0 \le F_{i,j,k,1} \le FU \end{array} \right] \tag{20}$$

$$f^{therm}(y_{i,j,k}, P_{i,j}, T_{i,j}) = 0 \tag{21}$$

$$f^{design}(\phi_{i,j,k}, P_{i,j}, T_{i,j}, V_{i,j}, \tau_{i,j,k,d,s,m}) = 0 \tag{22}$$

$$f^{hens}(QF_{i,j,d}, T_{i,j}, T^{s}_{i,j,d} P_{i,j}, z^{match}_{w,w}, z^{hot}_{w}, z^{cold}_{w}) = 0 \tag{23}$$

$$\underline{f}(z^{s}_{i,j,d,s,m}, z^{rx}_{i,j,c}, T^{min}) \le T_{i,j}, T^{s}_{i,j,d} \le \overline{f}(z^{s}_{i,j,d,s,m}, z^{rx}_{i,j,c}, T^{max}) \tag{24}$$

$$\underline{f}(z^{s}_{i,j,d,s,m}, z^{rx}_{i,j,c}, P^{min}) \le P_{i,j} \le \overline{f}(z^{s}_{i,j,d,s,m}, z^{rx}_{i,j,c}, P^{max}) \tag{25}$$

Here, Eqs. 1-4 are for material balances around each block. Eqs. 5-6 are for purity and demand constraints for the external product streams. Eq. 7 decomposes each flow rate term, $F_{i,j,k,d}$, as one positive and one negative counterpart. Eqs. 8-9 are for block energy balance and stream enthalpy definitions, respectively. In Eq. 9, several enthalpy terms are defined which correspond to enthalpy of streams at different locations. Eq. 10 is for determining the heat duties of the stream heater/coolers. Eq. 11 is to quantify the enthalpy change due to change in pressure. Eqs. 12-14 describe the material consumption/generation inside the block. Eq.14 determines whether a reaction is active in block $B_{i,j}$ or not. Eq. 15 states that each external product and jump product stream from block $B_{i,j}$ have the same composition, i.e. $y_{i,j,k}$. Eqs.16-20 describe the boundary assignments and determines the flow rate and composition of the

interblock streams. Eq.16 states that each boundary can be either unrestricted, semirestricted or completely restricted. If a boundary is selected as semi-restricted, then a phenomena or equipment is assigned through Eq. 17. Eq. 18 states that if a boundary is selected as unrestricted, then it has to comply with its source block composition. Eq. 19 and f^{sr} are for describing the specific separation operation assigned to semirestricted boundary. Eq.20 describes the zero flow condition for completely restricted boundary.

Eq. 21 represents the thermodynamic and reaction equilibrium relations ($f^{therm}(y_{i,j,k}, P_{i,j}, T_{i,j}) = 0$) that relate the physical attributes (temperature, pressure and composition) of a building block with its physical phase (liquid/vapor) and flow rates. Eq. 22 represents the models used for obtaining the equipment design variables and performing the equipment sizing calculations. Eq. 23 stands for heat integration model which is used to connect the stream and block heat duties with each other. Eqs. 24 and 25 are the bounds for block temperature, stream temperature and block pressure that can be a function of the phenomena or unit operations assigned to the block. A more detailed description of each of these constraints are given in the Supporting Information.

MINLP model P0 serves as a generic model for process integration, process synthesis and intensification. The common block equations that are needed in addressing different problem types are summarized in Figure 8. Material balances, energy balances, material generation/consumption and boundary formulations are common model elements in any type of the model. The description of reaction and semi-restricted boundary with f^{rxn} (Eq. 14) and f^{sr} (Eq. 19) are crucial in formulating different problems. f^{rxn} can be used to describe stoichiometric, equilibrium or kinetic models in ascending order of detail. Similarly, f^{sr} can be used to describe split fraction, equilibrium or rate-based models. For equipment-based process synthesis problems, semi-restricted boundary can be described through split fraction models. For process intensification, however, detailed rate-based or equilibrium models are required. This is crucial to identify the benefits that can be accrued from combining reaction and separation operations. This is demonstrated below with a rate-based description of a membrane operation. If the semi-restricted boundary is assigned as a gas separation membrane material, then the flow rate through it will depend on the partial pressure of the both permeate and retantate sides.

In building block representation, these are destination and source blocks for the semirestricted flow, respectively. Accordingly, a rate-based description of the semi-restricted boundary can be written as in Eq. 26. When reaction is also described through kinetic model, following constraints are obtained:

$$f^{sr}(y_{i,j,k}, T_{i,j}, P_{i,j}, T_{i,j+1}, P_{i,j+1}, y_{i,j,k}) = \lambda_{i,j,k,d,s,m}(P_{i,j}y_{i,j,k} - P_{i,j+1}y_{i,j+1,k})A_{i,j,d,s,m} \qquad \forall i,j,k,(s,m) \in SM \tag{26}$$

$$f^{rxn}(T_{i,j}, P_{i,j}, y_{i,j,k}, V_{i,j}) = kp_r exp(-\frac{Ea_r}{RT_{i,j}}) \prod_{k' \in kin} f(P_{i,j}, y_{i,j,k'})V_{i,j}\gamma_{r,k} \qquad i \in I, j \in J, k \in K, (r,c) \in RXC \tag{27}$$

$\lambda_{i,j,k,d,s,m}$ is the permeance of the membrane material and $A_{i,j,d,s,m}$ is the membrane area. kp_r is the pre-exponential factor, Ea_r is the activation energy, R is the gas constant, $f(P_{i,j}, y_{i,j,k'})$ is a function determining the concentration dependence of the rate expression based on the pre-specified inlet components $k_1, ..., k^*$. $V_{i,j}$ stands for the reaction volume, catalyst weight, surface area, etc. If the kinetic reaction model described via Eq. 27 is activated in either side of the semirestricted boundary, then the block compositions, i.e. $y_{i,j,k}$, is a common variable between the boundary model and reaction model, and, synergy between those two can be captured. With this, modeling of reactive separation operations can be achieved. Synergy between reaction and separation operations can be also captured through equilibrium-based reaction and semi-restricted boundary models. These models are elaborated in Supporting Information together with simpler split fraction and stoichiometric models.

[Figure 8 about here]

By utilizing different elements of P0, process synthesis, integration, and intensification problems can be formulated as shown in Figure 9. The simplest type of model is when building blocks are considered as sinks/sources for certain material properties. In this case, a mass integration problem can be formulated based on material balances satisfying source/sink demands and boundary formulations describing the splitting operations:

$$\begin{aligned} \max \quad & TAP \\ \text{s.t.} \quad & \text{Eqs. } 1-7, 15-16, 18, 20 \end{aligned} \tag{P1}$$

Model P1 can be extended with heat integration model to realize simultaneous mass and heat integration. In this case, block and stream energy balances are also introduced:

$$\begin{aligned} \max \quad & TAP \\ \text{s.t.} \quad & \text{Eqs. } 1-10, 15-16, 18, 20, 23 \end{aligned} \tag{P2}$$

Thermodynamics constraints can be also included in model P2 to describe phase change and/or two-phase streams as part of the heat integration model. When pre-specified equipment are introduced into the problem with boundary unit and block unit formulations, a process synthesis problem can be formulated as follow:

$$\begin{aligned} \max \quad & TAP \\ \text{s.t.} \quad & \text{Eqs. } 1-20, 22, 24-25 \end{aligned} \tag{P3}$$

In P3, the representation is based on equipment representation and Eqs.14 and 19 are described through stoichiometric and split fraction models. If needed, thermodynamics, kinetic and equilibrium reactor models can be also introduced. With the addition of heat integration constraints, simultaneous process synthesis and heat integration can be also addressed. Enabling process intensification, however, requires more detailed description of reaction and block boundaries. This also necessitates the use of thermodynamics constraints. Accordingly, process synthesis incorporating process intensification can be addressed with the following model:

$$\begin{aligned} \max \quad & TAP \\ \text{s.t.} \quad & \text{Eqs. } 1-20, 21, 24-25 \end{aligned} \tag{P4}$$

Here, Eq. 14 needs to incorporate either kinetic or equilibrium reaction models. Eq. 19 is required to be in the form of rate-based or equilibrium models to enable process intensification. Heat integration constraints can be also added to model P4 to enable simultaneous process synthesis, integration, and intensification. As objective function, following general expression

can be utilized:

$$
\begin{aligned}
\max \quad TAP = & \sum_{i\in I}\sum_{j\in J}\sum_{k\in K}\sum_{p\in PS} SP_{k,p}P_{i,j,k,p} - \sum_{i\in I}\sum_{j\in J}\sum_{k\in K}\sum_{f\in FS} UF_f M_{i,j,k,f} \\
& - \sum_{i\in I}\sum_{j\in J}\sum_{d\in D}\sum_{s,m\in SM} \kappa(z^s_{i,j,d,s,m}\mu_{s,m} + h^{sep}(N^{sep}_{i,j,d,s,m})) \\
& - \sum_{i\in I}\sum_{j\in J}\sum_{c\in CAT} \kappa(z^{rxn}_{i,j,c}\mu_c + h^{rxn}(N^{rxn}_{i,j,c})) \\
& - \sum_{i\in I}\sum_{j\in J}\sum_{d\in D} \kappa(h^{hex,cap}(Q^F_{i,j,d}, T_{i,j}, T^s_{i,j,d})) - \sum_{i\in I}\sum_{j\in J}\sum_{d\in D} UC(h^{hex,op}(Q^F_{i,j,d})) \\
& - \sum_{i\in I}\sum_{j\in J}\sum_{d\in D} \kappa(h^{pres,cap}(W^F_{i,j,d})) - \sum_{i\in I}\sum_{j\in J}\sum_{d\in D} EC(h^{pres,op}(W^F_{i,j,d}))
\end{aligned} \tag{28}
$$

Here, the first term corresponds to the revenue obtained from the product streams with selling price $SP_{k,p}$. The second term is the cost of raw materials with unit price UF_f. The third term is for determining the capital cost of the boundary operations. The fourth term stand for the capital cost of the block operations. Fifth and sixth terms are for determining the operating and capital cost of the heaters/coolers, respectively. Last two terms stand for the operating and capital cost of the pressure manipulator units. κ is the capital recovery factor. UC and UE are the unit price for the hot/cold utilities and electricity, respectively. With these models, building block representation and the corresponding mathematical model becomes a generic tool for process synthesis, integration, and intensification. In the next section, use of these models are demonstrated through a case study on ethylene glycol production.

[Figure 9 about here]

4 Case Study

In this section, an example problem on production of ethylene glycol is solved via building block superstructure approach to demonstrate the benefit of the tools introduced in the previous section. Ethylene glycol (EG) is an important chemical used as an antifreeze in automobiles, desiccant for natural gas production, and a raw material for the production of polyester fibers and resins.[59] Its industrial production is mainly based on the reaction of ethylene oxide (EO)

with water (W). Further reaction between the reactant EO and product EG results in diethylene glycol (DEG) production:

$$\begin{array}{rc} \text{Main Reaction:} & C_2H_4O + H_2O \rightarrow C_2H_6O_2 \\ \text{Side Reaction:} & C_2H_4O + C_2H_6O_2 \rightarrow C_4H_{10}O_3 \end{array}$$

Heavier glycols, e.g. tri-ethylene glycol, are also possible via side reactions between glycol products. The side reaction between EO and EG and the other side reactions producing heavier glycols can be avoided if high water content is introduced into the reactor.[60] This, however, results in high separation costs as the excess amount of water needs to be removed before high purity EG can be obtained. To show different aspects of the developed framework, this problem is first solved as a traditional process synthesis problem in which an equipment-based representation is used. Then, on the same problem, sequential and simultaneous heat exchanger network synthesis is demonstrated. Finally, a transition to the phenomena-based representation is made for obtaining intensified process flowsheets for the same problem.

4.1 *Process Synthesis*

In this section, how building block superstructure can be used to address superstructure-based synthesis problems is demonstrated. Equipment-based representation (as shown in Figure 4) and optimization formulation given with P3 is used to solve this problem. For reaction, kinetic reaction model with data from Altiokka and Akyalcin[61] is used. This implies that each building block with reaction operations correspond to a CSTR unit. Several different reactor configurations including CSTRs-in-series and PFR reactors are considered as different reactor alternatives. For the product purification, distillation columns are utilized.[62,63] Here, each distillation column is represented as a single block with a semi-restricted boundary which designates the position of the bottoms stream. Flows through semi-restricted boundary are described based on split-fraction models which are kept as variable to optimize the recovery and purity of the top and bottom streams. The objective is to generate a flowsheet featuring minimum total annual cost of production for 25 kmol/h EG production with 99.8% (mol) purity. Reactor type and volume, total number of distillation columns, their reflux ratio, reboiler duty and area, condensor duty and area, column dimensions, product recovery and purity are among

the decision variables. Fenske-Underwood-Gilliland correlations[27] are used while optimizing the distillation columns. Note that, total annual cost includes raw material costs, i.e. EO ad water, utility costs, i.e. cooling water, steam and electricity, annualized capital costs for reactors, separation columns, recycle pumps and heat exchangers. Capital cost functions, design formulations and utility costs are taken from literature[9,27,64–68] and provided in the Supporting Information. Temperature and pressure bounds of the process are taken as 340–520 K and 1–36 bar, respectively.[63]

In addressing this problem through block superstructure, a grid size of 2×9 is considered as shown in Figure 10a. Reaction and separation operations are assigned to the separate positions on this grid. While reaction is allowed to be positioned within the first five columns (yellow blocks), separation blocks are allowed to be positioned on the last four columns (green blocks). These separators are only allowed to be positioned at the second row. Total number of separation columns are restricted to 4. This is achieved through allowing the semirestricted boundary at only the designated positions (shown in green color in Figure **??**a). These streams, if activated, denote the bottoms streams of the distillation columns and flow rates through these boundaries are determined according to the short-cut design correlations. If they are not chosen as semirestricted, then the unrestricted boundary relations (i.e. splitting constraints) are activated and the corresponding distillation column is bypassed. In this way, number of distillation columns required for product separation is determined. Connectivity within the flowsheet is increased by activating recycle streams from the potential separator blocks. These streams are all connected to the inlet block of the reaction region, i.e. $B_{1,6}$. While the recycle from the first potential separator block is achieved through a vertical interblock stream from block $B_{1,6}$, recycle streams from the other potential separator blocks are represented through jump streams. Furthermore, fresh raw materials are allowed to enter at any block excluding the separator blocks and final product withdrawal with 99.8% EG is only activated from the block $B_{2,9}$. Note that pressure of the selected units are also considered as decision variables. Hence, pumping units are activated for all these recycle streams to account for possible difference in pressures. Distillation column reboiler and condenser pressures are determined based on bubble point calculations. As the reactions are in liquid phase, a phase check is performed at the block

$B_{2,5}$ based on bubble point calculations. This liquid phase constraint is only considered at the exit block from the reaction region as the reactions are exothermic and the reacting mixture will be at its highest temperature at the outlet of the reaction zone where its likelihood for phase change is the highest. In solution of the problems, the separator located on $B_{2,9}$ was always active. First no capital cost for stream heaters/coolers are considered and all the separators except the one on $B_{2,8}$ are activated. Then binary variables related with the other separators are freed one by one in the subsequent two iterations. Finally, with this as initial solution, full problem with the stream heater/cooler capital costs are solved. Following this solution strategy yields global optimal solution for the presented case studies in Section 4.1. and 4.2.

First, a base-case with a single CSTR[65] is considered. Reaction is allowed in block $B_{2,5}$ only. Problem includes 341 continuous and 3 binary variables, 620 nonlinear terms and 977 constraints. The overall problem is solved with ANTIGONE[69] to optimality and the resulting block superstructure and its equivalent flowsheet representations are shown in Figure 10b-c (Alternative 1). In the resultant flowsheet, CSTR is followed by three distillation columns: First two columns are used to separate water from the reactor effluents and the top products are recycled back to the reactor. Third distillation column takes in mainly EG and DEG and yields EG as the top product with 99.8% purity. Process has an total annual cost of \$13.68 MM/year (Table 2). Single-pass conversion of EO in the CSTR is 39.9% and the selectivity of EG/DEG is 11.5 kmol EG/ kmol DEG. The recycle flow rate is very high which increases the water concentration in the reactor inlet. This results in higher selectivity towards EG. High recycle flow rate between separators and reactor also provides clue for a potential intensification opportunity. As indicated by Baldea,[32] process intensification can be observed as tight material integration and, in this case, reaction and separation operations can be combined in a single unit to obtain a reactive distillation system. This was also suggested by others for the EG production.[46,63,70,71] This intensified alternative will be investigated further with phenomena-based representation in Section 4.3.

[Figure 10 about here]

[Table 2 about here]

Next, different CSTR unit configurations are investigated. Number of blocks that can be assigned with reactors is increased to 6 ($B_{1,3}$ to $B_{2,5}$). In the solution, only 4 out of 6 blocks alowed to be assigned with reaction is active which suggests 4 CSTRs-in-series. Problem includes 485 continuous and 9 binary variables, 770 nonlinear terms and 1379 constraints. Resultant process flowsheet is shown in Figure 11a (Alternative 2). Number of active searator units are the same with flowsheet Alternative 1. Volume of these CSTRs hit to the lower bound specified for the CSTRs. Capital cost is increased compared to single CSTR case, but TAC decreases to \$13.15 MM/year (3.8% reduction) as shown in Table 2. Main contribution to this much decrease in cost is due to the reduction in the amount of fresh EO fed into the system. This is made possible by increased EO conversion, 50.4%, and EG/DEG selectivity, 15.1 kmol EG/kmol DEG. As is observed from this case, multiple CSTR system performs better than the single CSTR case with better control over the reactant concentrations and less degree of mixing. It is also known that plug-flow reactors (PFRs) are preferable to maintain a high concentration of reactants.[72] Next, this alternative is investigated.

For PFR representation, 10 blocks (at equal volume and pressure) are considered. This corresponds to a 10 CSTRs-in-series model. Problem includes 580 continuous and 3 binary variables, 897 nonlinear terms and 1661 constraints. Solution of this problem yields an optimal flowsheet with \$12.96 MM/year TAC (Alternative 3). Resulting block superstructure and its equivalent flowsheet representations are shown in Figure 11b-c 5.2% decrease in the TAC is obtained compared to Alternative 1 (Table 2). Block supertructure result features a distributed feed to the reactor suggesting a differential side stream reactor (DSR). To understand the effect of distributed feed, problem is also solved with no feed allowed into the reaction blocks. In this case, a process alternative with slightly higher TAC is obtained (\$12.97 MM/year) (Alternative 4). It should be noted that DSR and PFR cost functions are assumed to be the same in this problem. Although PFR results in \$4,900 more cost, this might not justify the construction of a DSR with additional inlet ports. The objective of this case study is, however, to show that developed block superstructure representation and corresponding model can identify such complex reactor structures. Also, the same problem can be addressed simultaneously with PFR and multiple CSTR alternatives by considering a larger block superstructure. Solution of this

simultaneous problem does not yield any better solution.

[Figure 11 about here]

4.2 *Process Synthesis and Integration*

Material integration is already considered through recycle streams in the previous problem. Here, heat integration alternatives are investigated with building block superstructure representation. Only the integration between the distillation columns is considered. As PFR configuration resulted in lower TAC than the CSTRs, we will consider PFR as the reactor and we will not consider DSR configuration. In flowsheet Alternative 4, isothermal streams from distillation column reboilers and condensors can be integrated. A superstructure for the resulting Heat exchanger network synthesis (HENS) problem can be constructed through the building block-based approach with the heat integration representation shown in Figure 6c and as described in detail in Li et al.[55] However, there are only two streams that can be matched in this flowsheet: Bottoms of Sep1 and distillate of Sep3. Hence, there is no need to address this problem through a superstructure-based approach. Instead, we will address the HENS and process synthesis problem simultaneously. Here, representation stays the same and heat duties of the reboilers and condensers are allowed to be integrated with each other (Model is provided in Supporting Information). Problem includes 544 continuous and 9 binary variables, 933 nonlinear terms and 1590 constraints. Solution of this problem yields an optimal flowsheet with \$12.42 MM/year TAC (Figure 12b - Alternative 5). Unlike the not integrated one, this flowsheet contains four distillation columns. Operating pressure of the Sep1 is increased to 12 bar. Hence, it can operate at a higher temperature while performing a much sloppier water separation. This is compensated by the use of an additional column for EG/water separation. With these changes, annualized capital cost increases, but hot utility consumption decreases by 31% and cold utility consumption decrease by 29%. In overall, 4.2% decrease in the TAC is obtained compared to the non heat-integrated PFR alternative (Table 2). With this heat integration scheme, Alternative 5 resembles the industrial EG production process which also includes three columns for water/EG separation as described by Dye.[62]

[Figure 12 about here]

4.3 *Process Synthesis, Integration and Intensification*

In this section, intensification of the EG production problem is addressed through the optimization model P4. Here, we will explore several different flowsheet alternatives that cannot be identified with pre-specified unit operations as it was the case in the previous case studies. To enable this, we adopt phenomena-based representation. Accordingly, semi-restricted boundaries will be used to represent V-L phase contact phenomena (as described in Figure 3) rather than a whole pre-specified unit. First, we address the optimal heat integrated flowsheet obtained from Section 4.2 and consider it as a base-case structure for the further analysis of the problem. Phenomena-based representation of this flowsheet (Figure 12b) can be obtained within a 14×9 grid size as shown in Figure 13. Here, the first column ($j = 1$) contains the PFR which is represented as 10 CSTRs-in-series. Each pair of the remaining grid columns are used to represent a distillation unit. Required number of rows is given by the number of theoretical stages. For instance, the first distillation column (Sep1 in Figure 12)requires 3 theoretical stages including a partial reboiler. Hence, 2 rows of vapor-liquid block pairs, i.e. (blocks $B_{2,2}$ to $B_{3,4}$), can be used to represent these trays with equilibrium model. Then, blocks $B_{1,2}$ and $B_{1,3}$ are assigned as total condenser and blocks $B_{4,2}$ and $B_{4,3}$ are assigned as partial reboiler. The remaining distillation columns are also represented in a similar manner. To compare the solutions obtained from equipment-based and phenomena-based representations, we fix the reactor volume, reactor and distillation column pressures to the values obtained from equipment-based representation. Similarly, we provide lower bounds for the reflux ratios from the equipment-based solution. Problem includes 1137 continuous variables, 2248 constraints and 2971 nonlinear terms and solution with BARON for 6 hours of CPU time yields TAC of \$12.35 MM/year (18.1% optimality gap) which is lower than the one obtained with equipment-based representation, i.e. \$12.42 MM/year. And the difference between the two results mainly due to the hot utility consumption. Hot utility cost is 9.4% lower with the phenomena-based rigorous model. Now, we will explore several different flowsheet alternatives while using this result as the base-case. For simplicity, we will first solve several different flowsheet alternatives for minimization of the total annual

operating cost (TOC) and only consider capital cost of the in the objective if a promising flowsheet candidate is identified.

[Figure 13 about here]

With model P4 and phenomena-based representation, numerous eccentric flowsheets can be generated. For a smaller grid size, this was demonstrated in Demirel et al.[50] However, if this model is utilized with 14×9, model P4 becomes a large-scale MINLP with many nonlinear terms which cannot be addressed with current commerical solvers. Hence, here, we adopt a guided approach through fixing several structural decisions beforehand and generate and screen different intensified alternatives with reduced model sizes.

[Figure 14 about here]

We observed from the previous results that recycle flow rates from the separation columns to the reactors are very high. This indicates that reaction and distillation operations can be combined in a single reactive distillation unit as is also indicated in Section 4.1. We first investigate a single reactive distillation column to perform the given conversion and separation simultaneously. However, using 14 building block pairs (a grid size of 14×2) to represent and solve this problem do not provide a feasible solution. To investigate further, we increased the grid size to 100×2 and solved the problem for maximizing EG purity in the product. This corresponds to a reactive distillation column with 98 equilibrium trays. Solution of this problem yields 96.3% of purity, significantly less than 99.8% EG purity target. Hence, a second separation stage needs to follow this reactive distillation unit for feasible operation. To investigate this alternative, first four columns of the building block superstructure given in Figure 13 is utilized. This gives rise to a grid size of 14×4 (Figure 14). In this structure, Liquid (to the first and third columns of the grid) and vapor phase (to the second and forth columns of the grid) are fixed and the boundary between two phases are designated as vapor-liquid equilibrium boundary. Reaction is only allowed to be assigned to the first column of the grid (Blocks $B_{1,1}$ to $B_{14,1}$). Accordingly, blocks $B_{1,1}$ to $B_{14,2}$ represent a reactive distillation column and blocks $B_{1,3}$ to $B_{14,4}$ represent a distillation column. We solve this problem with BARON for 6 CPU hours for minimizing

total annual operating cost (Alternative 2). Problem includes 1052 continuous variables, 1778 constraints and 2204 nonlinear terms. Solution of this block superstructure yields a flowsheet with \$12.19 MM/year (21.3% optimality gap). This is significantly higher than the annual operating cost of the base case flowsheet, i.e. 5.3%.

[Figure 15 about here]

[Table 3 about here]

Can the reactive distillation operation be made more favorable? To investigate different design alternatives, we remove several constraints that are used to assign the building block aggregations as pre-specified equipment. One such constraint dictates that pressure of the building blocks around the vapor-liquid boundaries should be the same which ensures that the resulting structure can be translated as a single distillation column. Furthermore, we do not include any cost for pressure change operations. When we solve this problem for minimizng total annual operating cost, a building block result with \$11.99 MM/year is obtained (Figure 15a-c) (Alternative 3). As there is no cost associated with pressure change, there exists multiple pressure changes throughout the block superstructure. There are several separate reactive vapor-liquid equilibrium regions followed by non-reactive phase equilibrium regions. The reactive separation blocks operate at higher temperature and pressure than the non-reactive separation blocks which operate at the lowest allowed pressure, i.e. 1 atm. A flowsheet alternative that can realize this block superstructure result is given in Figure 15c. It includes 10 different equipment with pumps, compressors, expanders and valves in between. With this number of equipment and multiple pressure and temperature change operations, this flowsheet is not favorable. However, by judging from this building block result, we can propose a new flowsheet. As reactive V-L sections require high pressure and non-reactive V-L sections require low pressure, reactive distillation column can be separated into two separate units that can operate at different pressures. Accordingly, we introduce a third distillation column between the two distillation columns used before as shown in Figure 16a. We solve this problem with BARON for 6 hours with minimizing the TOC as objective. Problem includes 1916 continuous variables, 3009 constraints and 3903 nonlinear terms. This yields a solution with \$11.94 MM/year (19.6% optimality gap) (Alternative 4).

The resultant flowsheet is shown in Figure 16b. As expected, result improved compared to the two-column reactive distillation system, yet TOC is still higher than the flowsheet Alternative 1. However, we can further enhance the energy utilization and observe the benefits that can be accrued from heat integration. Accordingly, we investigate a possible integration between the condenser of the reactive distillation column and the second distillation column (Alternative 5). We solve this problem with BARON for 6 hours with minimizing the TOC as objective. Problem includes 1918 continuous variables, 3012 constraints and 3903 nonlinear terms. This yields a solution with \$11.53 MM/year (16.9% optimality gap) The resultant flowsheet is shown in Figure 16c. This result is slightly better than the TOC of the flowsheet alternative 1. Hence, we investigate this flowsheet further with TAC minimization. While doing so, we also investigate several different block superstructure sizes and change the number of rows for the superstructure shown in Figure 16a between 8 and 16. The best solution is obtained with a block superstructure size of 10 rows (Alternative 6). This flowsheet alternative is shown in Figure 17. The TAC of the optimized flowsheet is \$12.32 MM/year (20.7 % optimality gap) which is slightly better than the Flowsheet Alternative 1. Yet, this flowsheet includes only 3 units instead of 5 as in flowsheet alternative 1.

[Figure 16 about here]

[Figure 17 about here]

Although cost savings from this final flowsheet featuring a heat-integrated reactive distillation system is not drastic, 40% reduction in the number of equipment provides a novel intensification pathway. Note that, this alternative could not be identified with an equipment-based representation as is demonstrated in Section 4.1. and 4.2 even the problems could be solved to optimality. These higher level representations can be utilized to enhance the process performance for a given number of alternatives. However, identification of novel structures requires a lower level representation as is shown here. This also highlights the benefit of phenomena-based building block representation in systematic process intensification.

5 Conclusions

In this work, a novel building block superstructure and an MINLP-based model are put forward to address traditional process synthesis and integration problems while enabling intensification. Various unit operations and physiochemical phenomena are emulated using blocks in a two-dimensional grid which results in a systematic method for incorporation of process intensification in superstructure-based optimization. To demonstrate, ethylene glycol production problem is first solved as a superstructure-based synthesis problem with unit operation-based representation. Within the proposed unified method, simultaneous considerations are also possible. This is shown via an example on simultaneous process synthesis and heat exchanger network synthesis. Finally, ethylene glycol process is analyzed with phenomena-based representation with simultaneous consideration of intensified/non-intensified alternatives with heat and mass integration. Although reactive distillation alone did not result in a favorable process alternative, it is found that there exists intensified schemes that can enhance the performance of reactive distillation through heat integration. A final flowsheet with 40% reduction in number of equipment is obtained while achieving the same process performance. With these, the proposed representation provides a foundation for simultaneous synthesis, integration and intensification.

Acknowledgments

The authors gratefully acknowledge support from the U.S. National Science Foundation (award number CBET-1606027), the American Chemical Society Petroleum Research Fund (ACS PRF 58764-DNI9), and the DOE RAPID Institute.

Supporting Information

The details on the elements of model P0, capital and operating cost parameters. This information is available free of charge via the Internet at http://pubs.acs.org.

References

(1) Li, X.; Kraslawski, A. Conceptual process synthesis: past and current trends. *Chemical Engineering and Processing: Process Intensification* **2004**, *43*, 583–594.

(2) Siirola, J. J.; Rudd, D. F. Computer-aided synthesis of chemical process designs. From reaction path data to the process task network. *Industrial & Engineering Chemistry Fundamentals* **1971**, *10*, 353–362.

(3) Seader, J.; Westerberg, A. A combined heuristic and evolutionary strategy for synthesis of simple separation sequences. *AIChE Journal* **1977**, *23*, 951–954.

(4) Douglas, J. A hierarchical decision procedure for process synthesis. *AIChE Journal* **1985**, *31*, 353–362.

(5) Smith, R.; Linnhoff, B. The design of separators in the context of overall processes. *Chem. Eng. Res. Des* **1988**, *66*, 195–228.

(6) Smith, R. *Chemical process: design and integration*; John Wiley & Sons, 2005.

(7) Chen, Q.; Grossmann, I. Recent developments and challenges in optimization-based process synthesis. *Annual review of chemical and biomolecular engineering* **2017**, *8*, 249–283.

(8) Achenie, L.; Biegler, L. A superstructure based approach to chemical reactor network synthesis. *Computers & chemical engineering* **1990**, *14*, 23–40.

(9) Kokossis, A. C.; Floudas, C. A. Synthesis of isothermal reactorâĂŤseparatorâĂŤrecycle systems. *Chemical engineering science* **1991**, *46*, 1361–1383.

(10) Caballero, J. A.; Grossmann, I. E. Generalized disjunctive programming model for the optimal synthesis of thermally linked distillation columns. *Industrial & Engineering Chemistry Research* **2001**, *40*, 2260–2274.

(11) Linke, P.; Kokossis, A. Attainable reaction and separation processes from a superstructure-based method. *AIChE Journal* **2003**, *49*, 1451–1470.

(12) Onel, O.; Niziolek, A. M.; Elia, J. A.; Baliban, R. C.; Floudas, C. A. Biomass and natural gas to liquid transportation fuels and olefins (BGTL+ C2_C4): process synthesis and global optimization. *Industrial & Engineering Chemistry Research* **2015**, *54*, 359–385.

(13) Demirhan, C. D.; Tso, W. W.; Powell, J. B.; Pistikopoulos, E. N. Sustainable ammonia production through process synthesis and global optimization. *AIChE Journal* **2018**,

(14) El-Halwagi, M. M. *Pollution prevention through process integration: systematic design tools*; Elsevier, 1997.

(15) Klemeš, J. J.; Kravanja, Z. Forty years of heat integration: pinch analysis (PA) and mathematical programming (MP). *Current Opinion in Chemical Engineering* **2013**, *2*, 461–474.

(16) Jaksland, C. A.; Gani, R.; Lien, K. M. Separation process design and synthesis based on thermodynamic insights. *Chemical Engineering Science* **1995**, *50*, 511–530.

(17) Marquardt, W.; Kossack, S.; Kraemer, K. A framework for the systematic design of hybrid separation processes. *Chinese Journal of Chemical Engineering* **2008**, *16*, 333–342.

(18) Khorasany, R. M.; Fesanghary, M. A novel approach for synthesis of cost-optimal heat exchanger networks. *Computers & Chemical Engineering* **2009**, *33*, 1363–1370.

(19) Yuan, Z.; Chen, B.; Gani, R. Applications of process synthesis: Moving from conventional chemical processes towards biorefinery processes. *Computers & Chemical Engineering* **2013**, *49*, 217–229.

(20) Stankiewicz, A. I.; Moulijn, J. A. Process intensification: transforming chemical engineering. *Chemical engineering progress* **2000**, *96*, 22–34.

(21) Moulijn, J. A.; Stankiewicz, A.; Grievink, J.; Górak, A. Process intensification and process systems engineering: a friendly symbiosis. *Computers & Chemical Engineering* **2008**, *32*, 3–11.

(22) Bielenberg, J.; Palou-Rivera, I. The RAPID Manufacturing Institute âĂŞ Reenergizing US Efforts in Process Intensification and Modular Chemical Processing. *Chemical Engineering and Processing - Process Intensification* **2019**,

(23) Tian, Y.; Demirel, S. E.; ; Hasan, M. M. F.; Pistikopoulos, E. N. An Overview of Process Systems Engineering Approaches for Process Intensification: State of the Art. *Chemical Engineering and Processing: Process Intensification* **2018**, *133*, 160 – 210.

(24) Demirel, S. E.; Li, J.; Hasan, M. F. Systematic process intensification. *Current Opinion in Chemical Engineering* **2019 https://doi.org/10.1016/j.coche.2018.12.001**,

(25) Lutze, P.; Babi, D. K.; Woodley, J. M.; Gani, R. Phenomena based methodology for process synthesis incorporating process intensification. *Industrial & Engineering Chemistry Research* **2013**, *52*, 7127–7144.

(26) Karuppiah, R.; Grossmann, I. E. Global optimization for the synthesis of integrated water systems in chemical processes. *Computers & Chemical Engineering* **2006**, *30*, 650–673.

(27) Douglas, J. M. *Conceptual design of chemical processes*; McGraw-Hill New York, 1988; Vol. 1110.

(28) Wu, W.; Henao, C. A.; Maravelias, C. T. A superstructure representation, generation, and modeling framework for chemical process synthesis. *AIChE Journal* **2016**, *62*, 3199–3214.

(29) Henao, C. A.; Maravelias, C. T. Surrogate-based superstructure optimization framework. *AIChE Journal* **2011**, *57*, 1216–1232.

(30) Cozad, A.; Sahinidis, N. V.; Miller, D. C. Learning surrogate models for simulation-based optimization. *AIChE Journal* **2014**, *60*, 2211–2227.

(31) Balasubramanian, P.; Bajaj, I.; Hasan, M. M. F. Simulation and optimization of reforming reactors for carbon dioxide utilization using both rigorous and reduced models. *Journal of CO2 Utilization* **2018**, *23*, 80–104.

(32) Baldea, M. From process integration to process intensification. *Computers & Chemical Engineering* **2015**, *81*, 104–114.

(33) Ponce-Ortega, J. M.; Al-Thubaiti, M. M.; El-Halwagi, M. M. Process intensification: new understanding and systematic approach. *Chemical Engineering and Processing: Process Intensification* **2012**, *53*, 63–75.

(34) Pichardo, P.; Manousiouthakis, V. I. Infinite DimEnsionAl State-space as a systematic process intensification tool: Energetic intensification of hydrogen production. *Chemical Engineering Research and Design* **2017**, *120*, 372–395.

(35) Bertran, M.-O.; Frauzem, R.; Sanchez-Arcilla, A.-S.; Zhang, L.; Woodley, J. M.; Gani, R. A generic methodology for processing route synthesis and design based on superstructure optimization. *Computers & Chemical Engineering* **2017**, *106*, 892–910.

(36) Siirola, J. J. *Advances in chemical engineering*; Elsevier, 1996; Vol. 23; pp 1–62.

(37) Agreda, V. H.; Partin, L.; Heise, W. High-purity methyl acetate via reactive distillation. *Chemical Engineering Progres* **1990**, 40–46.

(38) Lutze, P.; Gani, R.; Woodley, J. M. Process intensification: a perspective on process synthesis. *Chemical Engineering and Processing: Process Intensification* **2010**, *49*, 547–558.

(39) Arizmendi-Sánchez, J. A.; Sharratt, P. Phenomena-based modularisation of chemical process models to approach intensive options. *Chemical Engineering Journal* **2008**, *135*, 83–94.

(40) Rong, B.-G.; Kolehmainen, E.; Turunen, I. *Computer Aided Chemical Engineering*; Elsevier, 2008; Vol. 25; pp 283–288.

(41) Freund, H.; Sundmacher, K. Towards a methodology for the systematic analysis and design of efficient chemical processes: Part 1. From unit operations to elementary process functions. *Chemical Engineering and Processing: Process Intensification* **2008**, *47*, 2051–2060.

(42) Kaiser, N. M.; Flassig, R. J.; Sundmacher, K. Reactor-network synthesis via flux profile analysis. *Chemical Engineering Journal* **2018**, *335*, 1018–1030.

(43) Babi, D. K.; Lutze, P.; Woodley, J. M.; Gani, R. A process synthesis-intensification framework for the development of sustainable membrane-based operations. *Chemical Engineering and Processing: Process Intensification* **2014**, *86*, 173–195.

(44) Babi, D. K.; Holtbruegge, J.; Lutze, P.; Gorak, A.; Woodley, J. M.; Gani, R. Sustainable process synthesis–intensification. *Computers & Chemical Engineering* **2015**, *81*, 218–244.

(45) Kuhlmann, H.; Veith, H.; MoÌĹller, M.; Nguyen, K.-P.; Górak, A.; Skiborowski, M. Optimization-Based Approach to Process Synthesis for Process Intensification: Synthesis of Reaction-Separation Processes. *Industrial & Engineering Chemistry Research* **2017**, *57*, 3639–3655.

(46) Papalexandri, K. P.; Pistikopoulos, E. N. Generalized modular representation framework for process synthesis. *AIChE Journal* **1996**, *42*, 1010–1032.

(47) Tian, Y.; Pistikopoulos, E. N. Synthesis of Operable Process Intensification Systems - Steady-State Design with Safety and Operability Considerations. *Industrial & Engineering Chemistry Research* **2019 DOI: 10.1021/acs.iecr.8b04389**,

(48) Wilson, S.; Manousiouthakis, V. IDEAS approach to process network synthesis: Application to multicomponent MEN. *AIChE journal* **2000**, *46*, 2408–2416.

(49) da Cruz, F. E.; Manousiouthakis, V. I. Process intensification of reactive separator networks through the IDEAS conceptual framework. *Computers & Chemical Engineering* **2017**, *105*, 39–55.

(50) Demirel, S. E.; Li, J.; Hasan, M. M. F. Systematic process intensification using building blocks. *Computers & Chemical Engineering* **2017**, *105*, 2–38.

(51) Li, J.; Demirel, S. E.; Hasan, M. M. F. Simultaneous Process Synthesis and Process Intensification using Building Blocks. *Computer Aided Chemical Engineering* **2017**, *40*, 1171–1176.

(52) Li, J.; Demirel, S. E.; Hasan, M. M. F. Process Synthesis using a Block Superstructure with Automated Flowsheet Generation and Optimization. *AIChE Journal* **2018**, *64*, 3082–3100.

(53) Demirel, S. E.; Li, J.; Hasan, M. F. Simultaneous process synthesis and heat integration using a single superstructure. *Computing and Systems Technology Division 2017 - Core Programming Area at the 2017 AIChE Annual Meeting* **2017**, *2017-October*, 199–200.

(54) Demirel, S. E.; Li, J.; Hasan, M. M. F. A General Framework for Process Synthesis, Integration and Intensification. *Computer Aided Chemical Engineering* **2018**, *44*, 445–450.

(55) Li, J.; Demirel, S. E.; Hasan, M. M. F. Process Integration Using Block Superstructure. *Industrial & Engineering Chemistry Research* **2018**, *57*, 4377–4398.

(56) Li, J.; Demirel, S. E.; Hasan, M. M. F. Fuel Gas Network Synthesis Using Block Superstructure. *Processes* **2018**, *6*, 23.

(57) Li, J.; Demirel, S.; Hasan, M. Building Block-Based Synthesis and Intensification of Work-Heat Exchanger Networks (WHENS). *Processes* **2019**, *7*, 23.

(58) Yee, T. F.; Grossmann, I. E.; Kravanja, Z. Simultaneous optimization models for heat integrationâĂŤIII. Process and heat exchanger network optimization. *Computers & chemical engineering* **1990**, *14*, 1185–1200.

(59) Yue, H.; Zhao, Y.; Ma, X.; Gong, J. Ethylene glycol: properties, synthesis, and applications. *Chemical Society Reviews* **2012**, *41*, 4218–4244.

(60) Rebsdat, S.; Mayer, D. Ethylene glycol. *Ullmann's Encyclopedia of Industrial Chemistry* **2000**,

(61) Altiokka, M. R.; Akyalcin, S. Kinetics of the hydration of ethylene oxide in the presence of heterogeneous catalyst. *Industrial & Engineering Chemistry Research* **2009**, *48*, 10840–10844.

(62) Dye, R. F. Ethylene glycols technology. *Korean Journal of Chemical Engineering* **2001**, *18*, 571–579.

(63) Barecka, M. H.; Skiborowski, M.; Górak, A. *Practical Aspects of Chemical Engineering*; Springer, 2018; pp 17–34.

(64) Seider, W. D.; Seader, J. D.; Lewin, D. R. *Product & Process Design Principles: Synthesis, analysis and evaluation*; John Wiley & Sons, 2009.

(65) Hamid, M. K. A.; Sin, G.; Gani, R. Integration of process design and controller design for chemical processes using model-based methodology. *Computers & Chemical Engineering* **2010**, *34*, 683–699.

(66) Luyben, M. L.; Luyben, W. L. Design and control of a complex process involving two reaction steps, three distillation columns, and two recycle streams. *Industrial & engineering chemistry research* **1995**, *34*, 3885–3898.

(67) Zhang, Q.; Liu, M.; Zeng, A. Performance enhancement of pressure-swing distillation process by the combined use of vapor recompression and thermal integration. *Computers & Chemical Engineering* **2019**, *120*, 30–45.

(68) Espatolero, S.; Romeo, L. M.; Cortés, C. Efficiency improvement strategies for the feedwater heaters network designing in supercritical coal-fired power plants. *Applied Thermal Engineering* **2014**, *73*, 449–460.

(69) Misener, R.; Floudas, C. A. ANTIGONE: algorithms for continuous/integer global optimization of nonlinear equations. *Journal of Global Optimization* **2014**, *59*, 503–526.

(70) Ciric, A. R.; Gu, D. Synthesis of nonequilibrium reactive distillation processes by MINLP optimization. *AIChE Journal* **1994**, *40*, 1479–1487.

(71) Jackson, J. R.; Grossmann, I. E. A disjunctive programming approach for the optimal design of reactive distillation columns. *Computers & Chemical Engineering* **2001**, *25*, 1661–1673.

(72) Fogler, H. S. *Elements of chemical reaction engineering*; Prentice-Hall International London, 2006.

List of Tables

List of Figures

Table 1: Aspects of process synthesis, integration and intensification.

	Process Synthesis	Process Integration	Process Intensification
Scale	Process equipment and flowsheet	Overall plant	Underlying phenomena, enabling materials
Focus	Flowsheet structure, equipment performance	Material and energy redistribution	Phenomena combination, enhancements
Emphasis	Equipment type and connectivity	Utility network connectivity	Phenomena, material type and connectivity
Models	High level, short-cut models	High level, short-cut models	Detailed models
Representation	Equipment network	Source-Sink network	Phenomena aggregations
Systematic Methods	Heuristic/hierarchical, optimization-based	Pinch analysis, optimization-based	Knowledge-based/heuristics, optimization-based

Table 2: Cost summary for the flowsheets generated through equipment-based process synthesis.

Flowsheet Alternative	Raw Material (MM$/year)	Hot Utility (MM$/year)	Cold Utility (M$/year)	TOC (MM$/year)	Capital (MM$/year)	TAC (MM$/year)
1	11.252	1.674	80.4	13.007	0.666	13.672
2	10.849	1.357	65.8	12.272	0.878	13.150
3	10.867	1.372	66.5	12.306	0.655	12.960
4	10.863	1.375	66.7	12.305	0.661	12.966
5	10.682	0.949	47.1	11.678	0.742	12.420

Table 3: Cost summary for the flowsheets generated through phenomena-based process synthesis.

Flowsheet Alternative	Raw Material (MM$/year)	Hot Utility (MM$/year)	Cold Utility (M$/year)	TOC (MM$/year)	Capital (MM$/year)	TAC (MM$/year)
1	10.704	0.860	43.1	11.612	0.736	12.347
2	10.795	1.335	64.8	12.194	-	-
3	10.755	1.176	57.5	11.989*	-	-
4	10.660	1.219	59.5	11.939	-	-
5	10.600	0.882	44.0	11.526	-	-
6	10.675	0.873	43.6	11.597	0.721	12.317

*Does not include all hot/cold utility and operating costs from compressors/pumps.

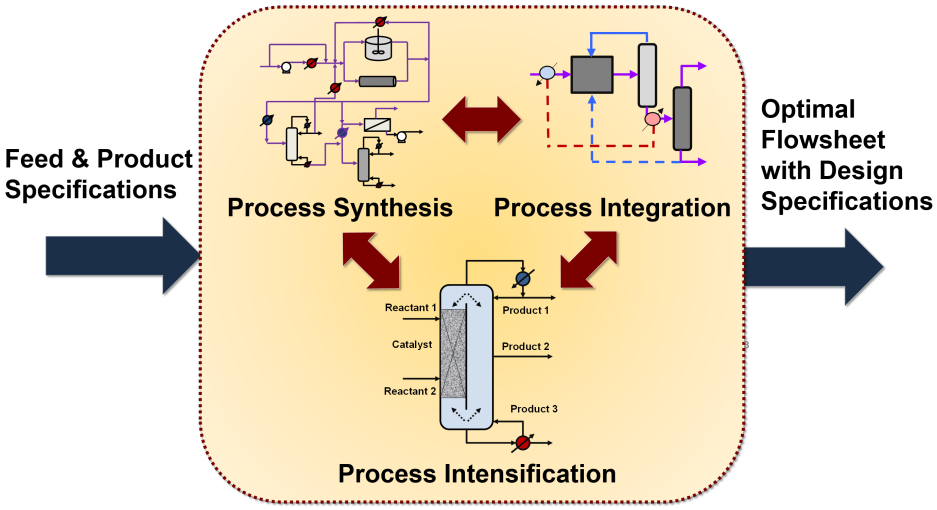

Figure 1: Conceptual process design methods for chemical processes.

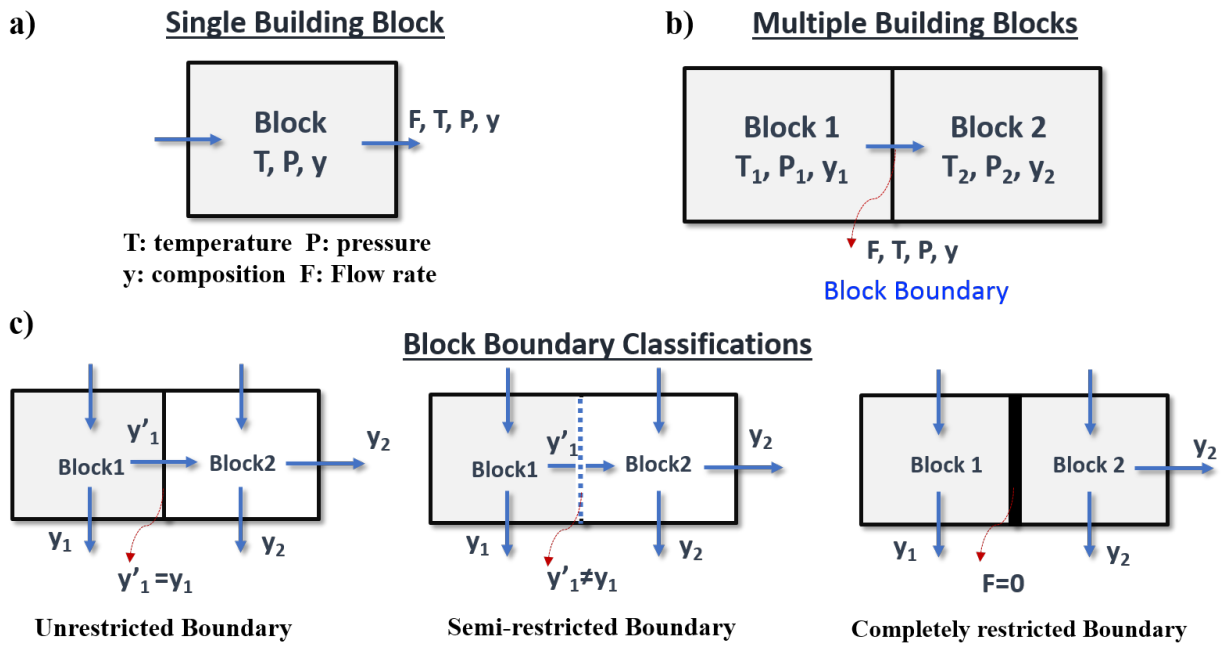

Figure 2: Building block representation. a) Single block with temperature, pressure and composition assignments, b) multiple blocks in which boundary classification becomes important, c) boundary classifications. Boundary between neighboring blocks can be either unrestricted, semi-restricted or completely-restricted.

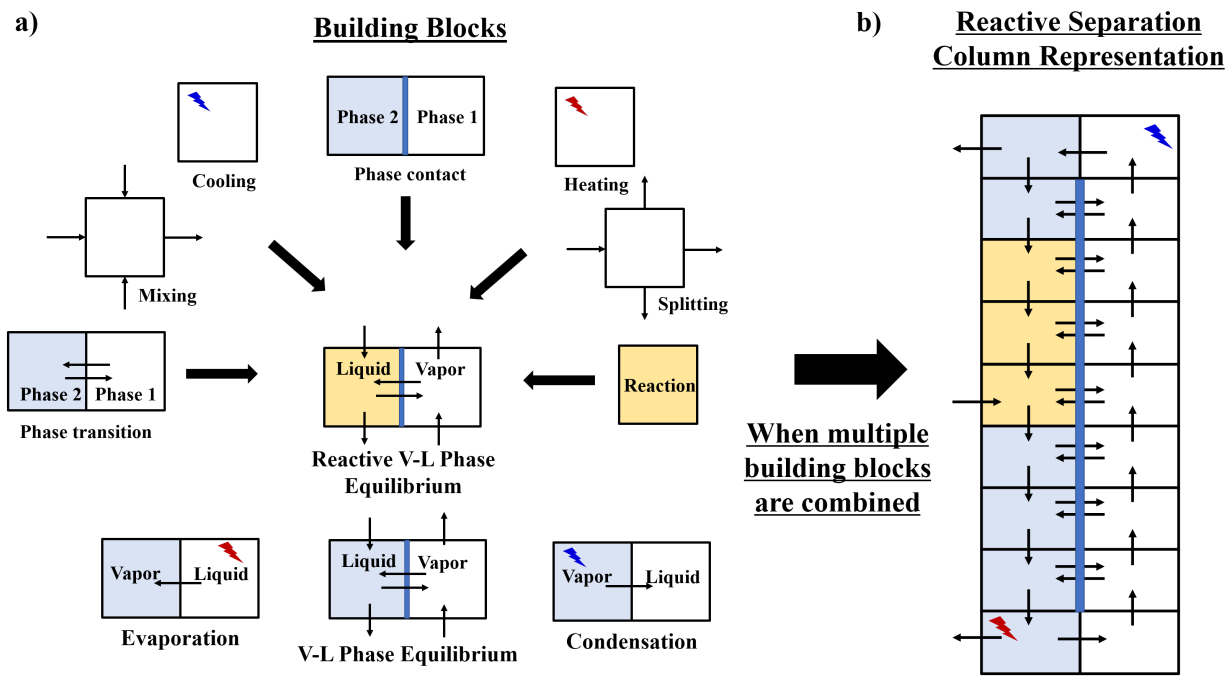

Figure 3: a) Phenomena descriptions based on building blocks. While some phenomena can be represented by single blocks, i.e. heating, cooling, mixing, splitting, some others require at least two neighboring building blocks. These basic descriptions can be combined in single or multiple blocks and different constituents of chemical processes, i.e. evaporation, condensation, reactive and non/reactive V-L equilibrium stages, can be represented. b) When these basic phenomena representations are connected to each other, a reactive separation column can be represented.

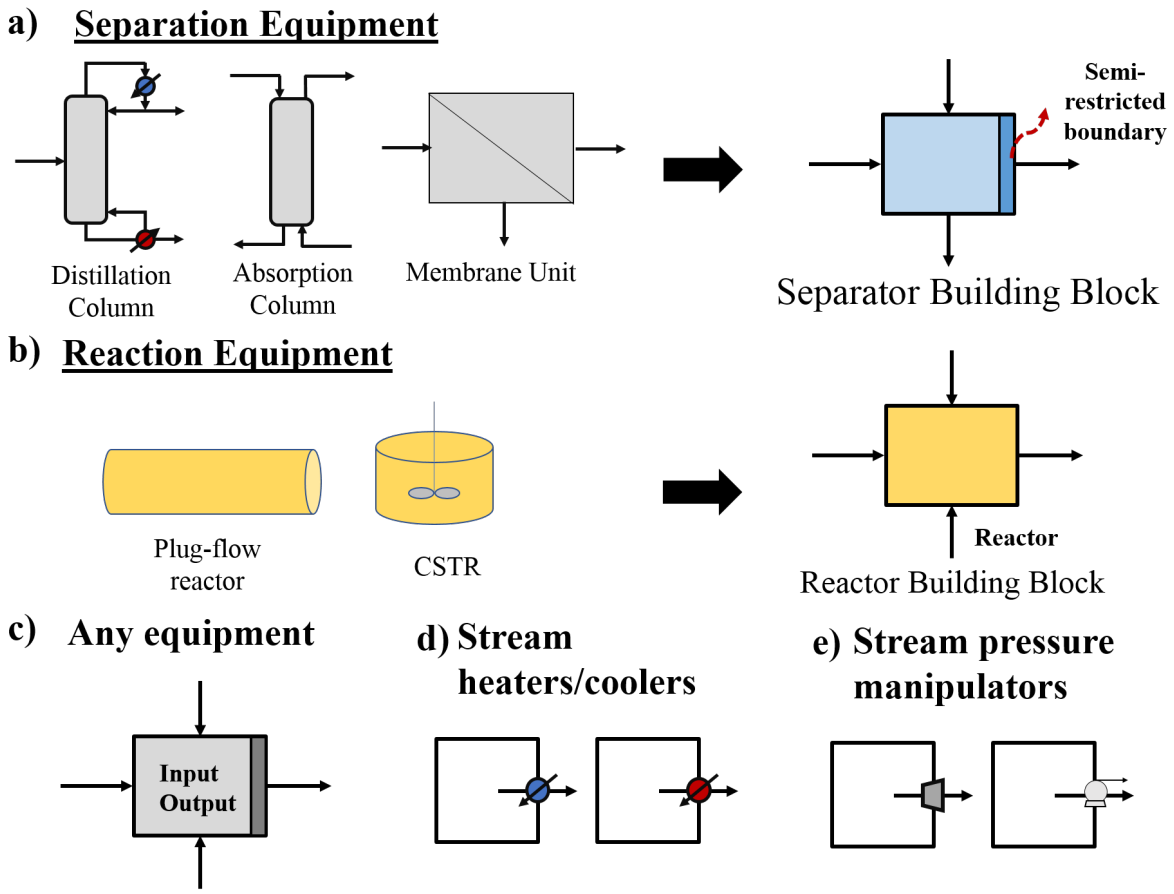

Figure 4: Equipment representations with building blocks. a) Different separation equipment can be represented through a single building block with semi-restricted boundary indicating the direction of one of the outlet (either lean or rich) streams, b) different reaction equipment and their building block representations, c) an equipment described by input-output models, d) stream heaters/coolers, and e) stream pressure manipulator units.

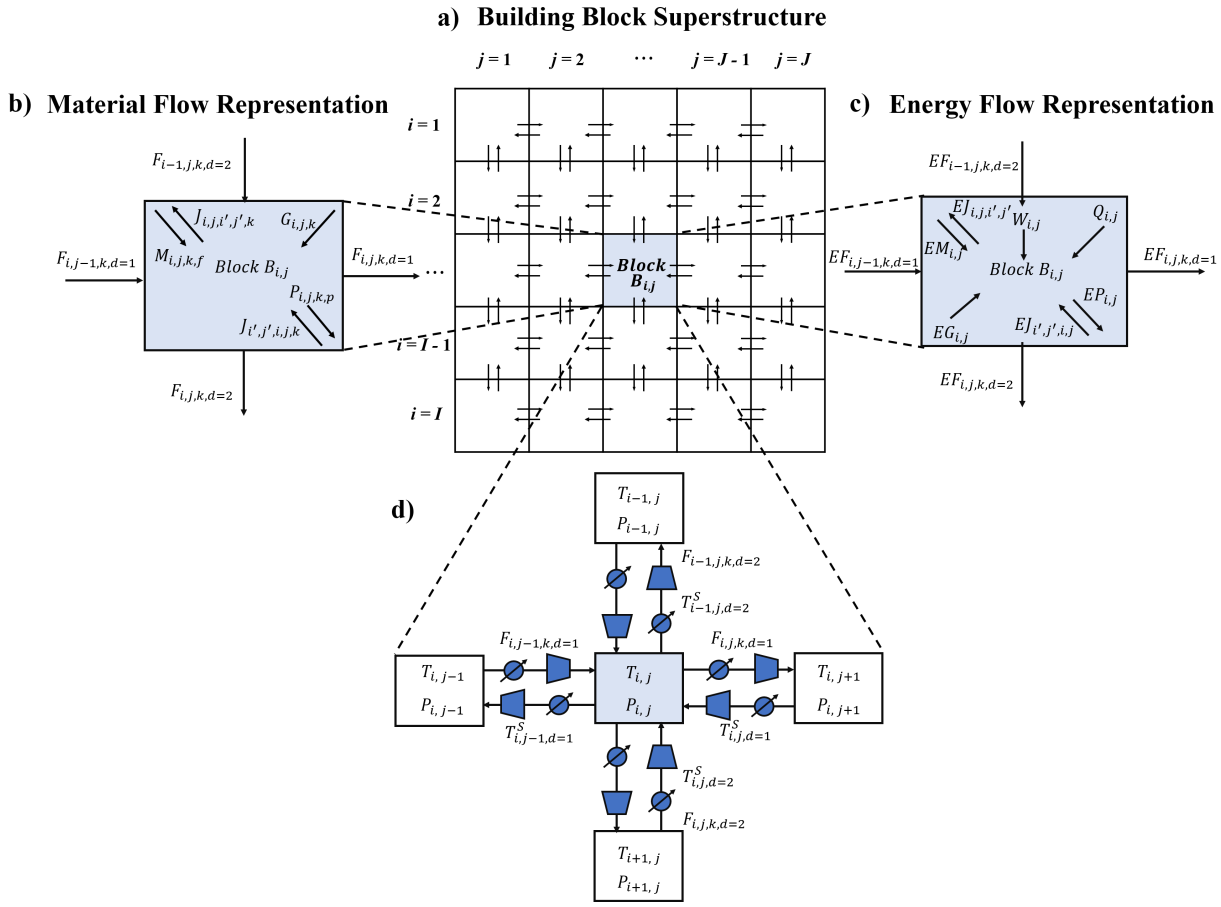

Figure 5: Building block superstructure. a) Generic building block superstructure representation is obtained by combining building blocks in a 2D arrangement, b) material flow representation and flow variables, c) energy flow representation and enthalpy variables, and d) stream heaters/coolers and pressure manipulator equipment representation. Note that these pressure manipulators are positioned after the stream heaters/coolers.

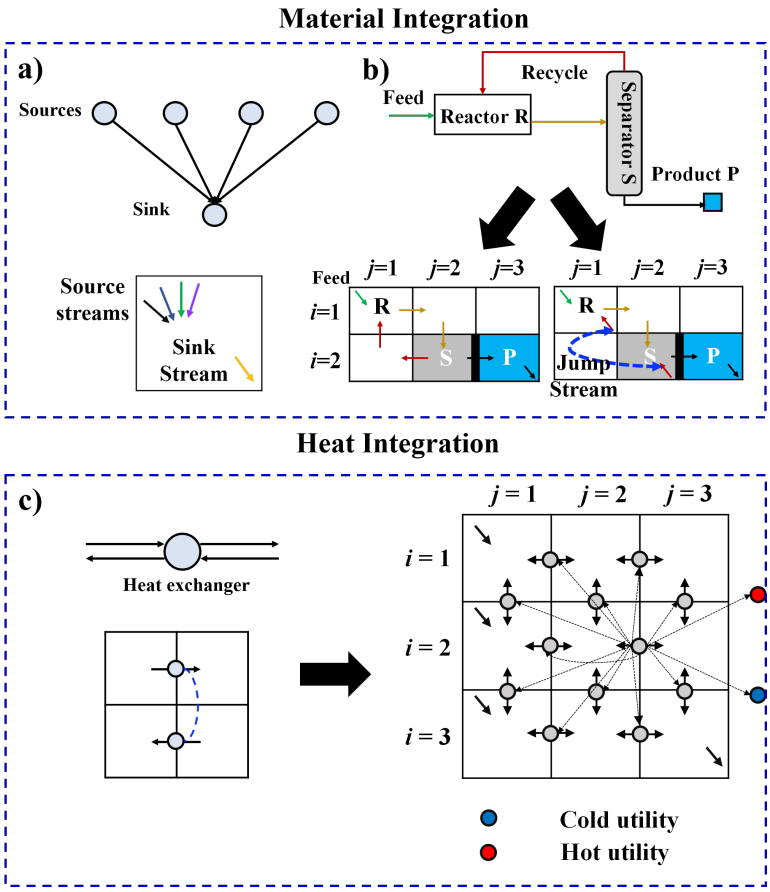

Figure 6: Building block superstructure representation for mass and heat integration. a) A source/sink network with four source streams and one sink can be represented by a single block with multiple feed streams, b) material integration in flowsheet level can be captured by bidirectional flow representation which is shown here for a reactor-separator-recycle system, c) heat exchangers are represented as virtual connections between any stream heaters/coolers. Any stream heater/cooler can either exchange heat with another stream in the superstructure or with external utility streams.

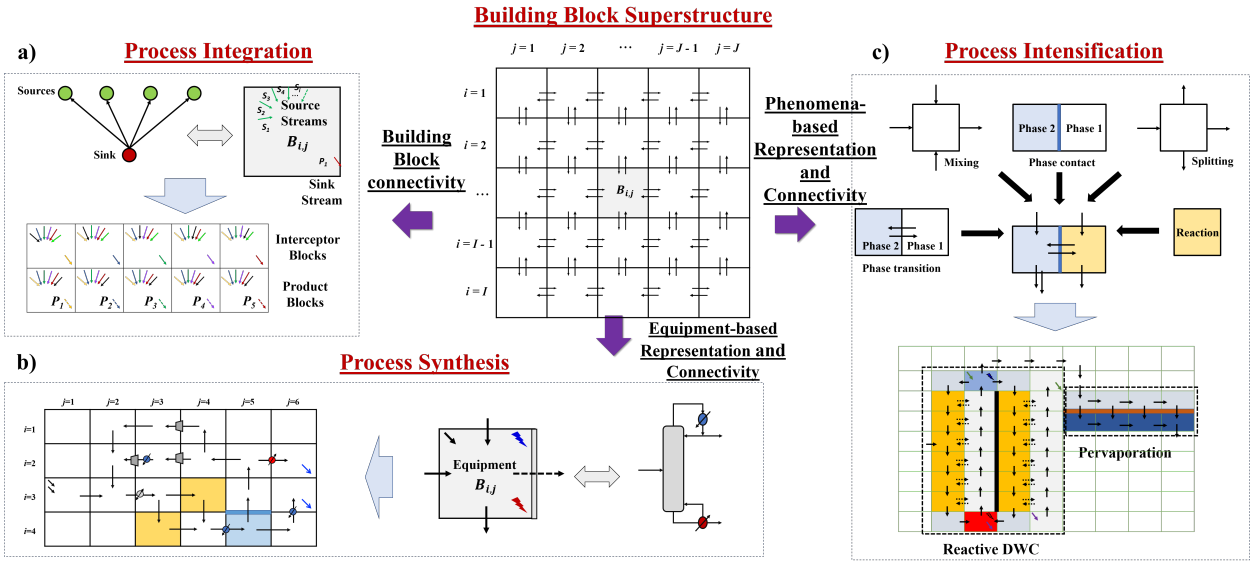

Figure 7: Building block representation for process integration, synthesis and intensification allows for addressing problems with different scales. a) Process integration representation, in which problems can be addressed merely by utilizing the connectivity within the superstructure, b) equipment-based representation, which allows for representation of traditional process synthesis superstructures, c) novel phenomena-based description of the processes, which allows to capture process intensification alternatives at the most fundamental level. As the representation scale gets lower, novel process design becomes possible.

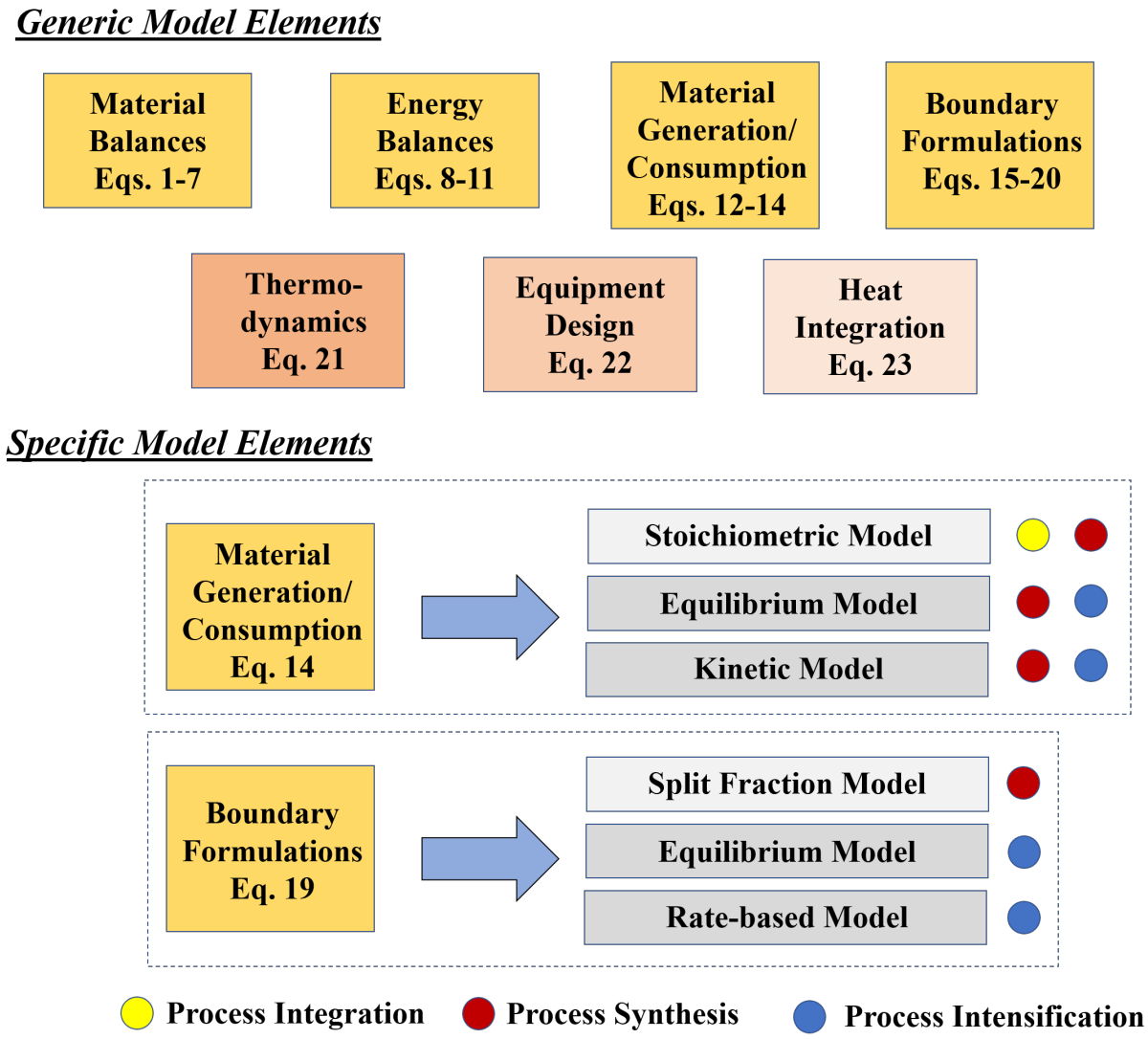

Figure 8: Components of the generic MINLP model. Key feature in determining the type of the problem addressed lies in how reaction and boundary formulations are addressed.

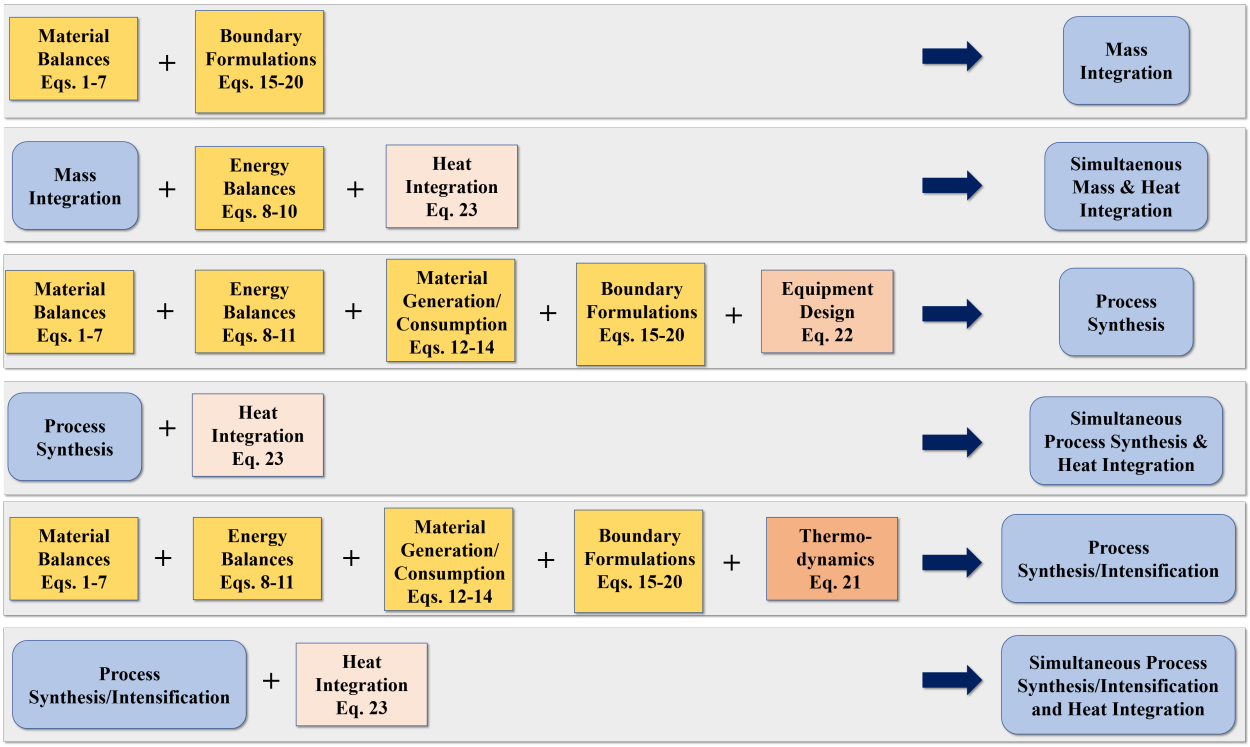

Figure 9: Through the generic modeling elements described in Figure 8, several different models can be derived.

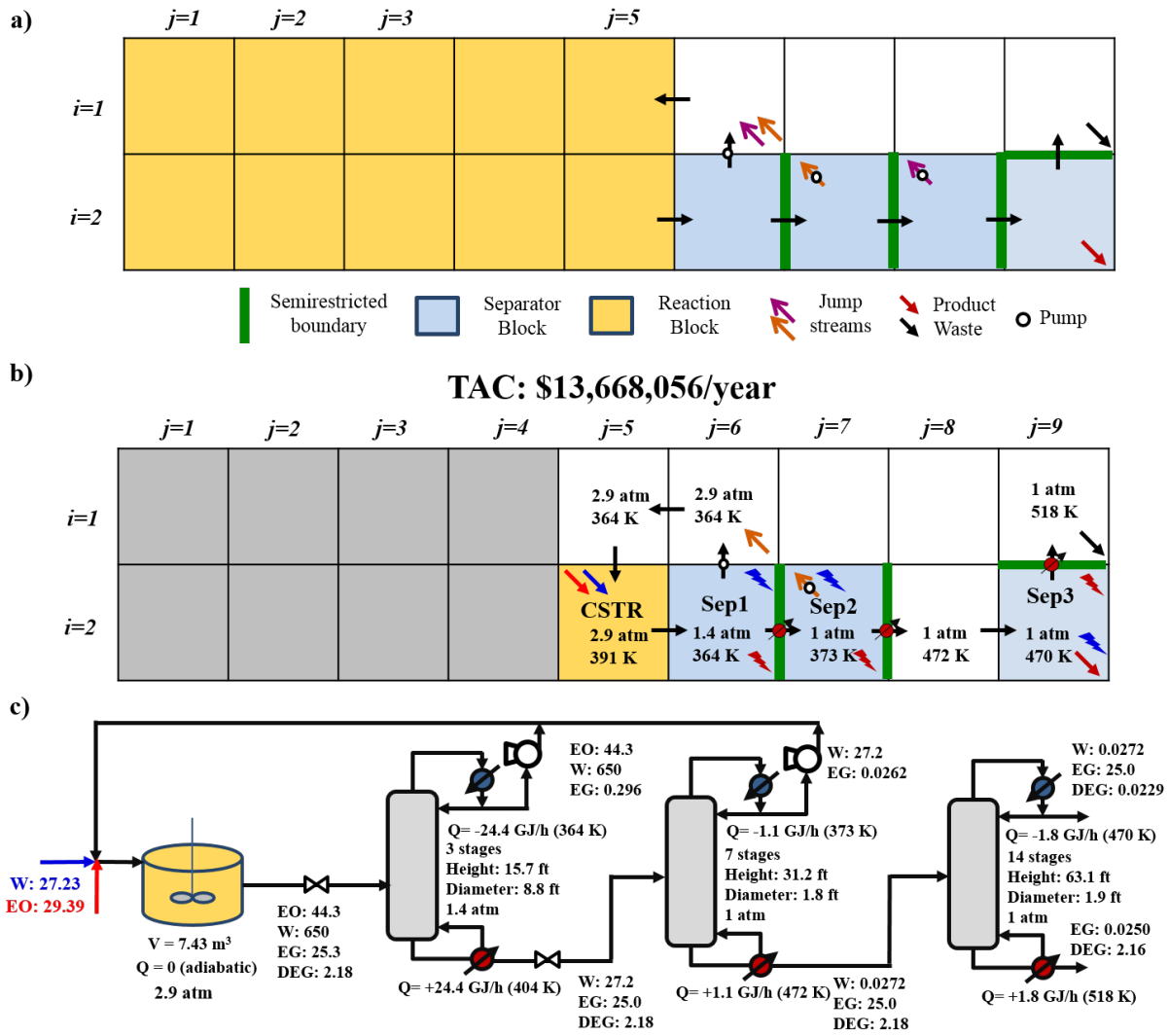

Figure 10: a) Process synthesis superstructure for ethylene glycol production, b) building block result for the flowsheet with single CSTR (Alternative 1), and c) equivalent flowsheet representation.

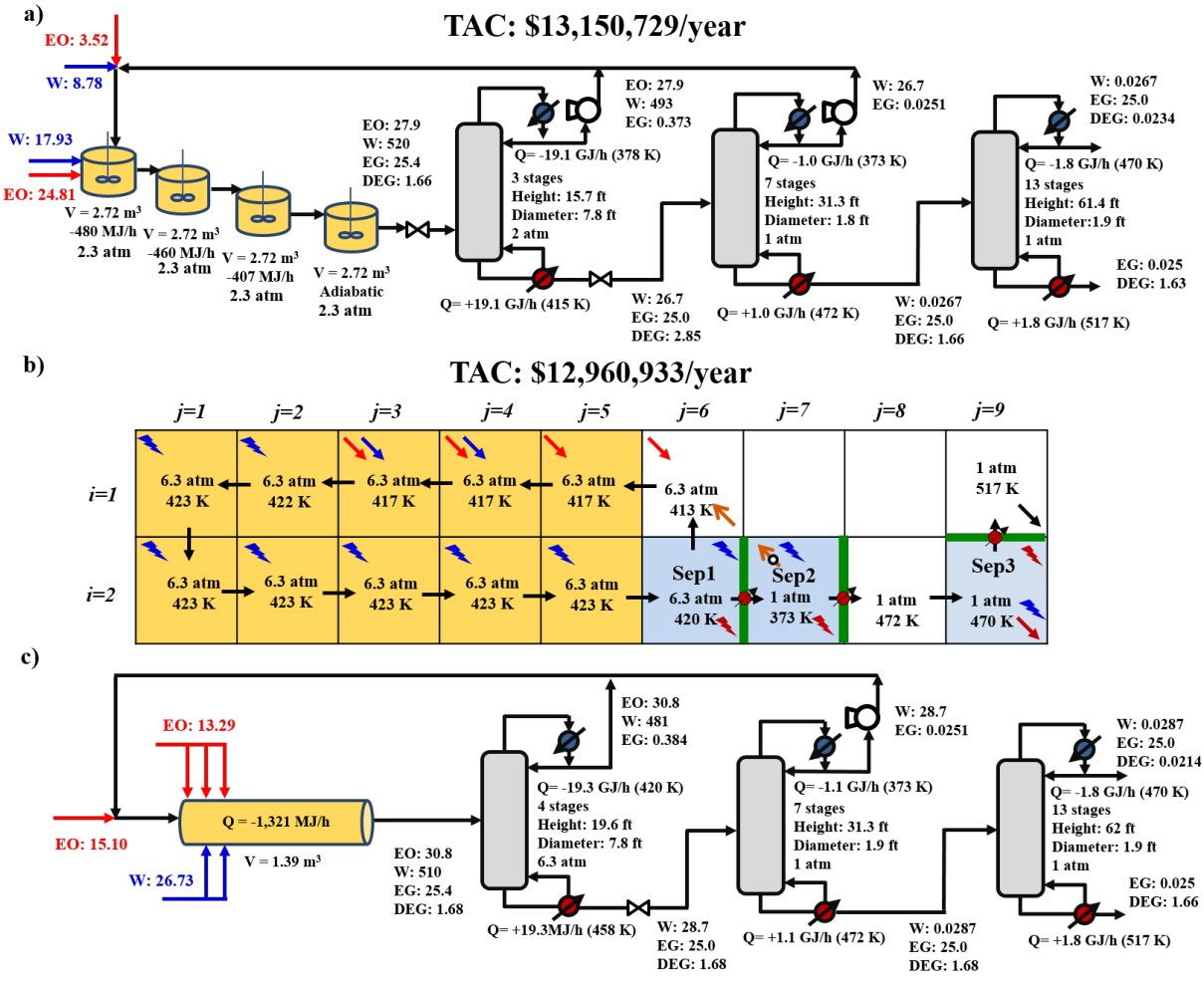

Figure 11: a) Flowsheet representation for the optimal result with multiple CSTRs (Alternative 2), b) building block result for the solution with PFR featuring a DSR (distributed side-stream reactor - Alternative 3), c) flowsheet representation of the optimal result with DSR.

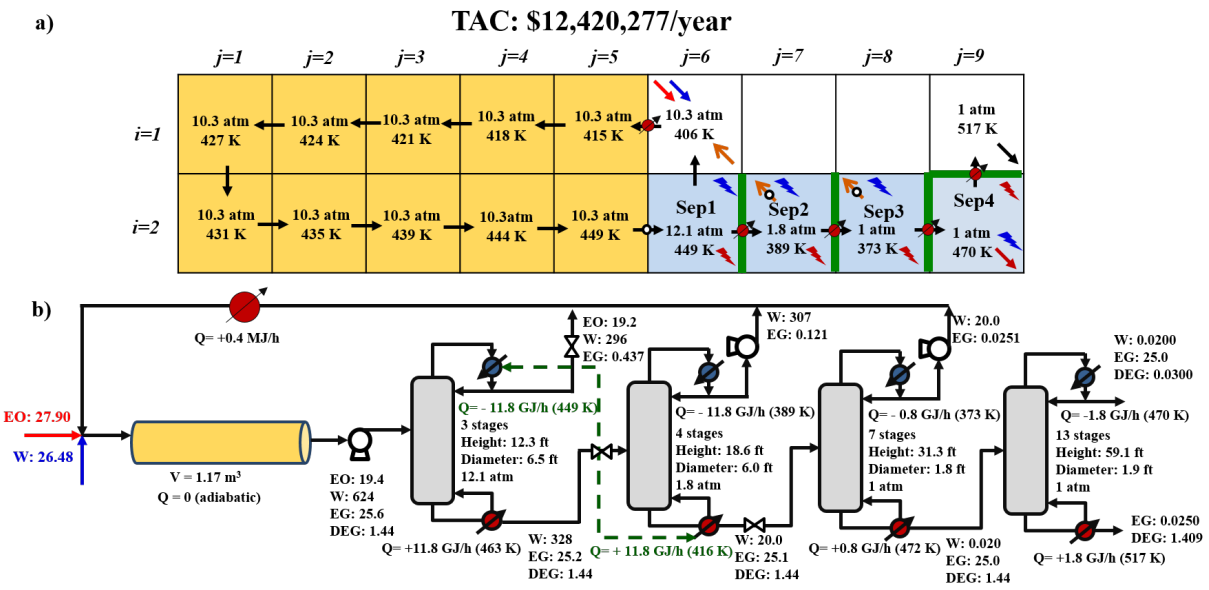

Figure 12: a) Building block superstructure result for the simultaneous process synthesis and HENS problem (Alternative 5), and b) corresponding flowsheet representation.

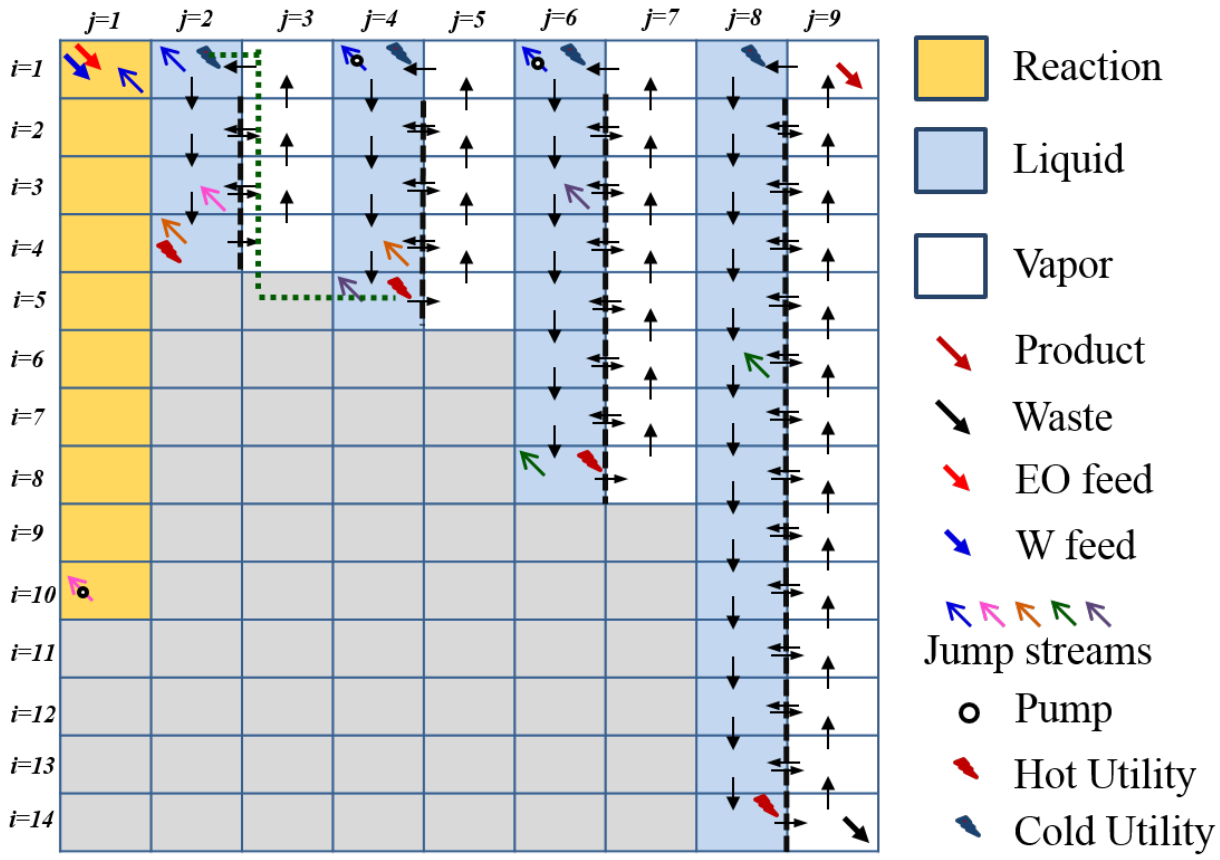

Figure 13: Phenomena-based representation of the optimal heat integrated flowsheet identified in Section 4.2.

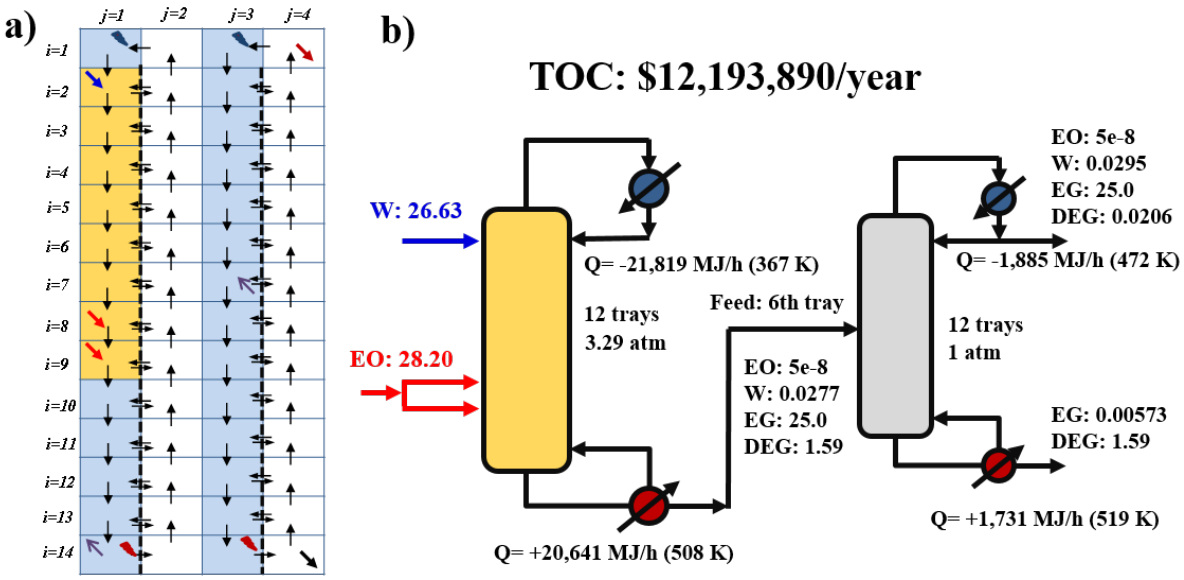

Figure 14: Flowsheet with reactive distillation followed by a distillation column. a) Building block superstructure result, b) corresponding flowsheet (Alternative 2).

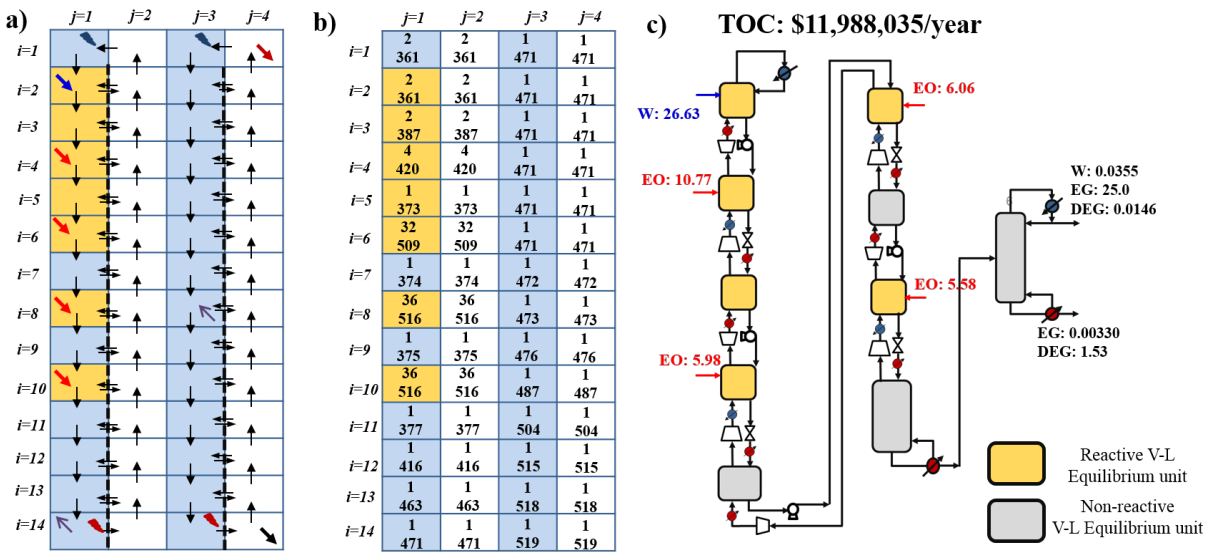

	j=1	j=2	j=3	j=4
i=1	2 361	2 361	1 471	1 471
i=2	2 361	2 361	1 471	1 471
i=3	2 387	2 387	1 471	1 471
i=4	4 420	4 420	1 471	1 471
i=5	1 373	1 373	1 471	1 471
i=6	32 509	32 509	1 471	1 471
i=7	1 374	1 374	1 472	1 472
i=8	36 516	36 516	1 473	1 473
i=9	1 375	1 375	1 476	1 476
i=10	36 516	36 516	1 487	1 487
i=11	1 377	1 377	1 504	1 504
i=12	1 416	1 416	1 515	1 515
i=13	1 463	1 463	1 518	1 518
i=14	1 471	1 471	1 519	1 519

Figure 15: Block superstructure result when equipment constraints related with pressure are removed. a) Block superstructure result, b) temperature and pressure of the building blocks, c) a flowsheet representation for this result containing several reactive and non-reactive V-L equipment with pressure manipulations in between (Alternative 3). This result shows that while reaction is favored at high pressure and temperature, separation of EG from the reaction products is favored at low pressure and temperature.

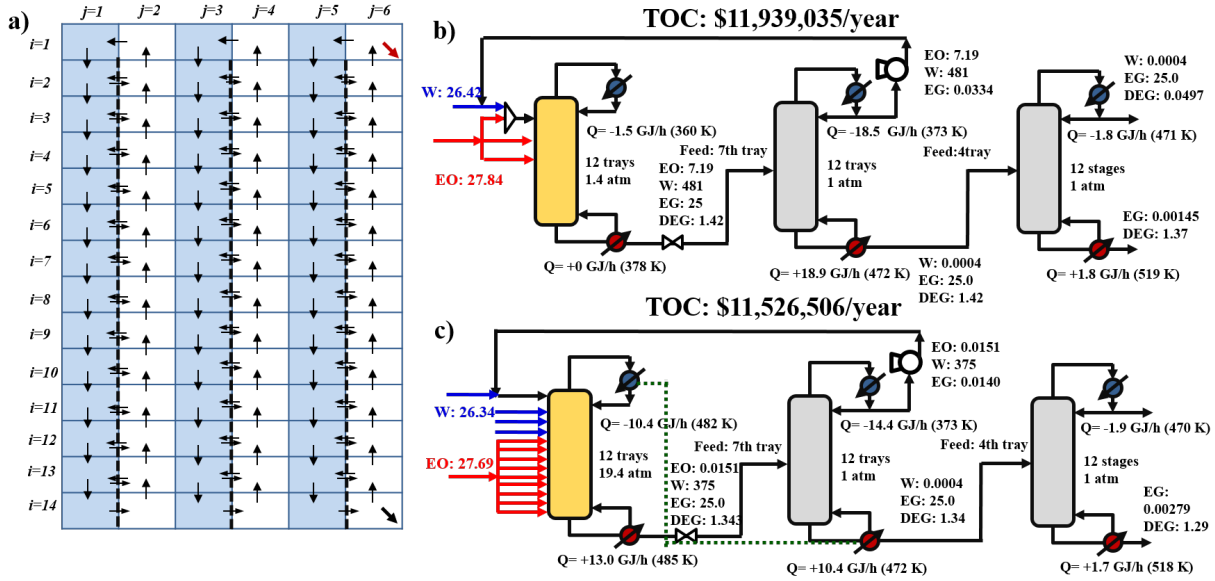

Figure 16: Flowsheet alternatives with 3 columns. a) Block superstructure representation used in obtaining these flowsheets, b) flowsheet Alternative 4 with RD followed by two non-reactive separation column operating at lower pressure, c) flowsheet alternative 5 with heat integration between the RD and the low-pressure column.

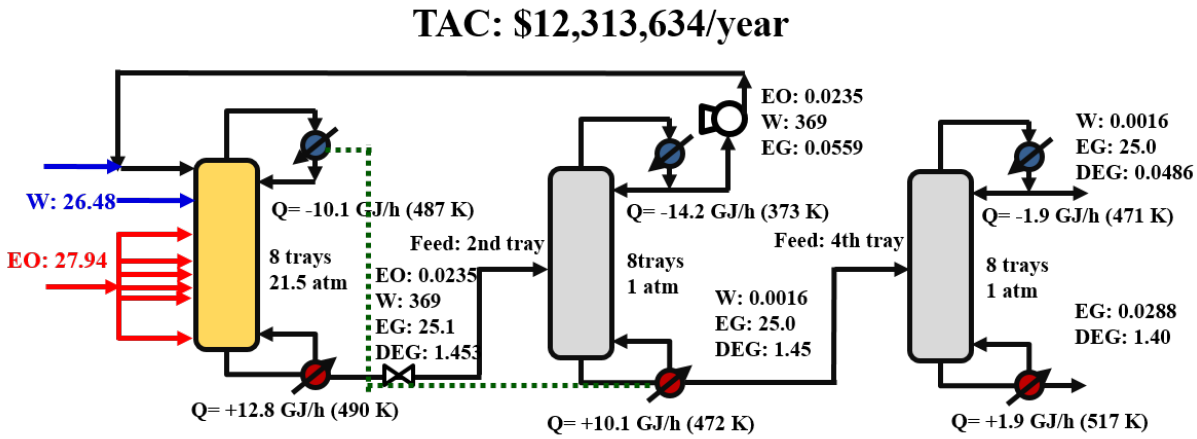

Figure 17: Flowsheet alternative 6 with minimum cost as objective